Production mechanisms of nuclear and hypernuclear clusters in relativistic ion collisions

Alexander Botvina, Marcus Bleicher
ITP/FIAS, Goethe University, Frankfurt am Main (Germany)

Nihal Buyukcizmeci
Selcuk University, Konya (Turkey)

2019 COST Action THOR Annual meeting
Istanbul Technical University, Istanbul, Turkey.
September 2-6 , 2019

Qualitative picture of dynamical stage of the reaction leading to fragment production (e.g., UrQMD calculations)

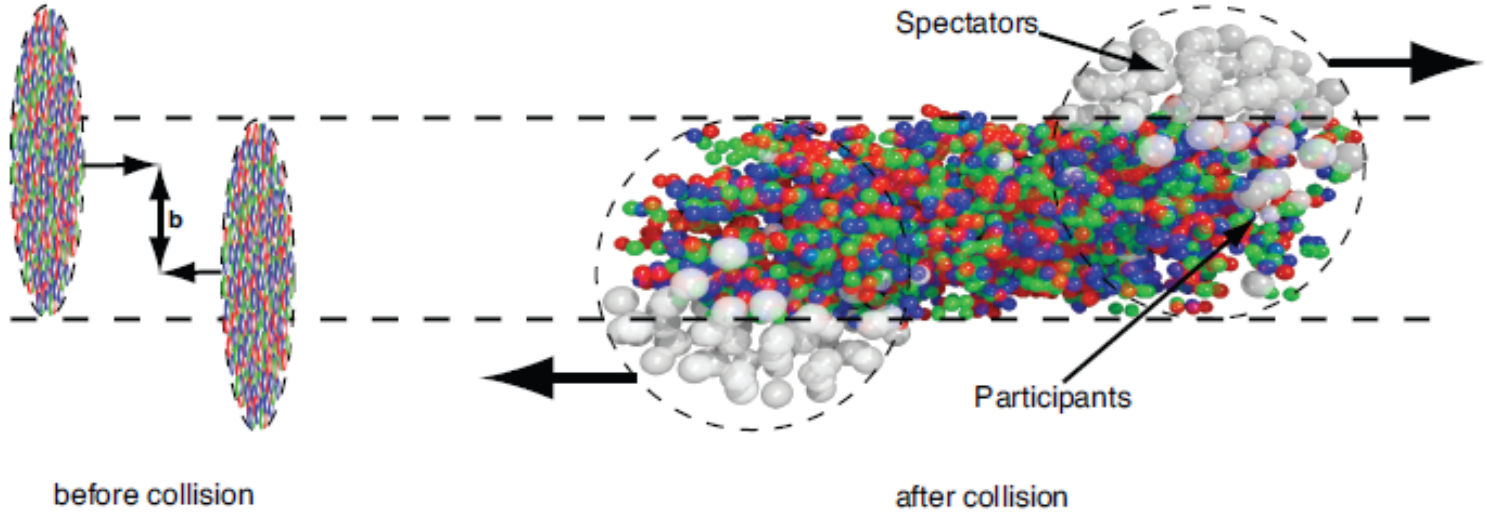

Fragment formation is possible from both participants and spectator residues

UrQMD PHSD DCM GiBUU

Production mechanisms of nuclear cluster species including anti-matter, hyper-matter in relativistic HI and hadron collisions:

- Production of all kind of particles (anti- , strange, charmed ones) in individual binary hadron collisions. Effects of nuclear medium can be included.
- Secondary interactions and rescattering of new-born particles are taken into account. (Looks as partial 'thermalization'.)
- Coalescence of all-possible baryons into composite (exotic, anti- , hyper-) nuclear species.
- Capture of produced baryons by big excited nuclear residues.

Statistical decay of excited nuclear species into new nuclei

- Multifragmentation into small nuclei (high excitations),
- Evaporation and fission of large nuclei (low excitations),
- (Fermi-) Break-up of small nuclei into lightest ones.

Long tradition of fragment measurements in high energy reactions:

Fragment production in Au+Au collisions: ALADIN (GSI) + Multics/Miniball (MSU) experiments

(G.J.Kunde et al., PRL 74, 38 (1995))

Difference of fragment yields obtained in spectator region (very broad distribution) and in central collisions (exponential fall of yields with mass/charge): Indication on different fragment production mechanisms.

Also there is a fragment flow in central collisions (high kinetic energies per nucleon respective to c,m, of decaying system).

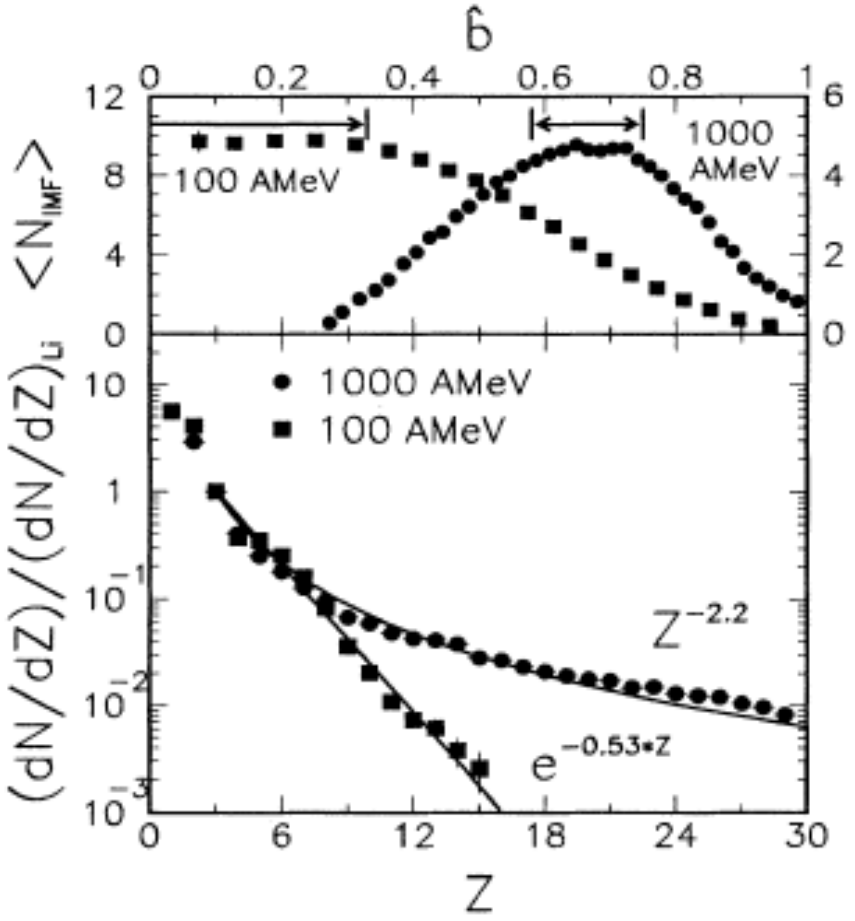

A mechanism for production of novel fragments: Capture of produced baryons by other nucleons and by spectator residues (nuclear matter)

Phenomenological models:

Coalescence of baryons

momenta:

$$|Pi - P0| \leq Pc$$

coordinates:

$$|Xi - X0| \leq Xc$$

Capture in nuclear potential and coalescence are similar mechanisms

Hyperon capture in the spectator potential

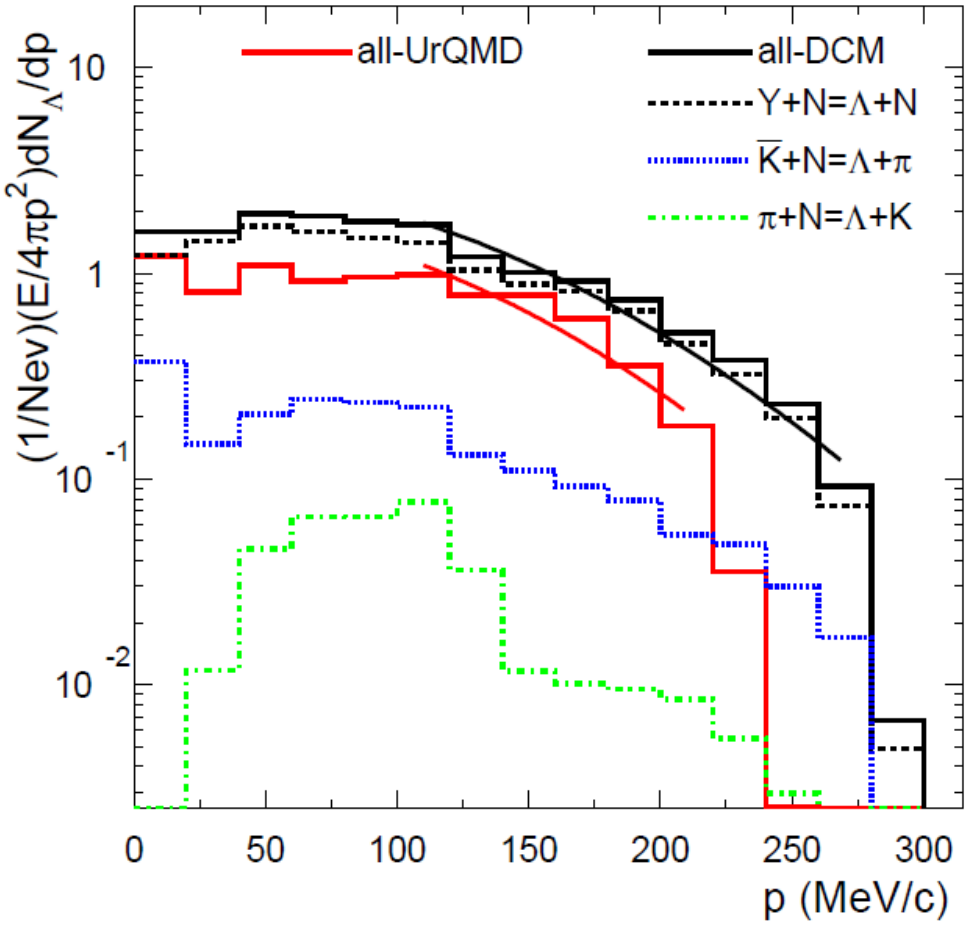

Au(20AGeV)+Au: UrQMD&DCM: PRC**84**, 064904 (2011)

Production of light nuclei in central collisions :

DCM, UrQMD, CB - Phys. Lett. B**714**, 85 (2012), Phys. Lett. B742, 7 (2015)

DCM versus experiment : coalescence mechanism

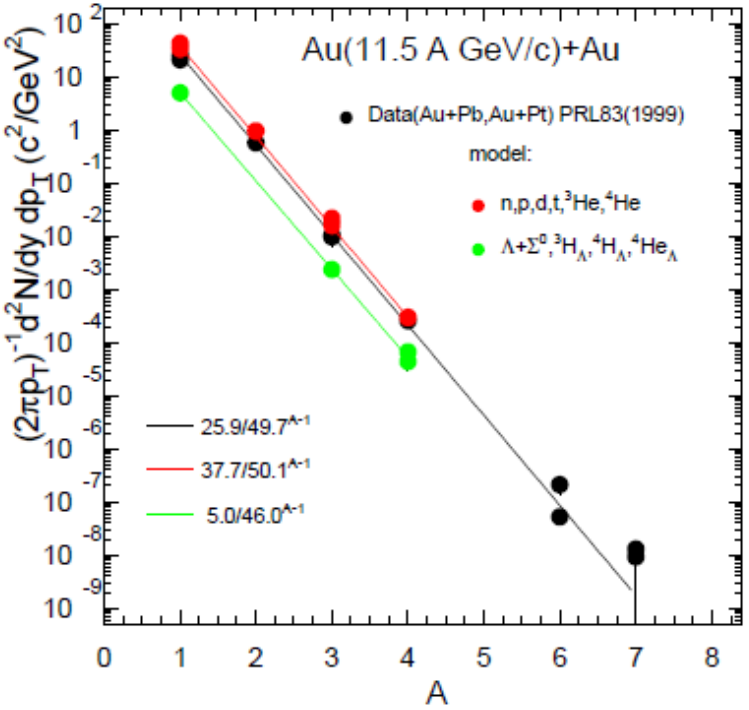

It is not possible to produce big nuclei !

Hybrid approach at LHC energies: UrQMD+hydrodynamics+coalescence

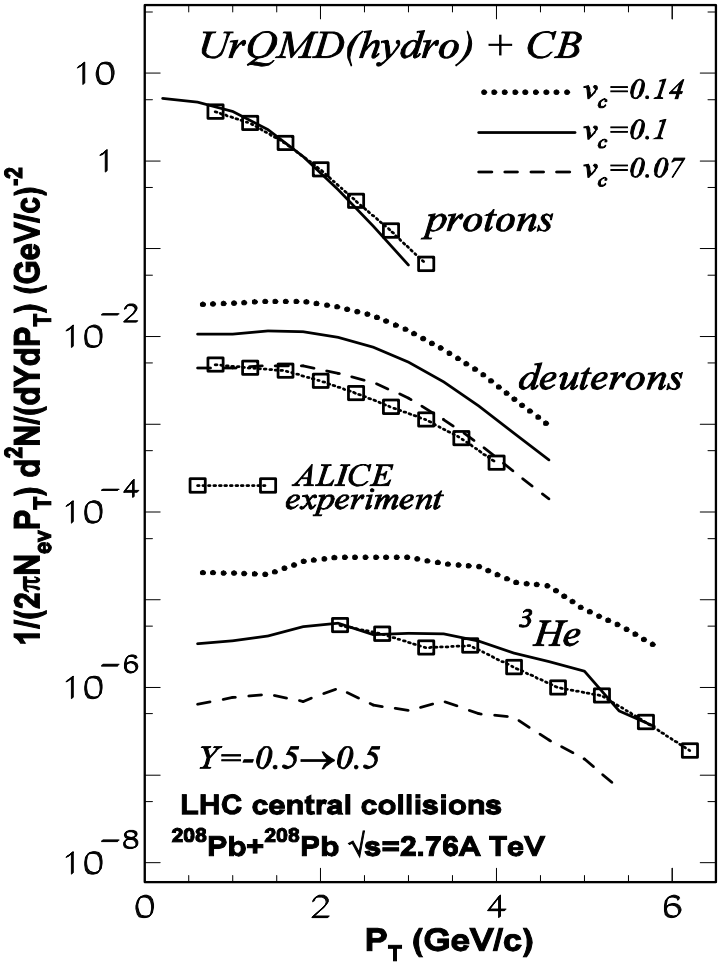

Phys. Rev. C96, 014913 (2017)

Charmed nuclei production at FAIR energies : coalescence ?
(try to find: no observation of such nuclei until now)

Steinheimer, Botvina, Bleicher : UrQMD + CB - Phys. Rev. C95, 014911 (2017)

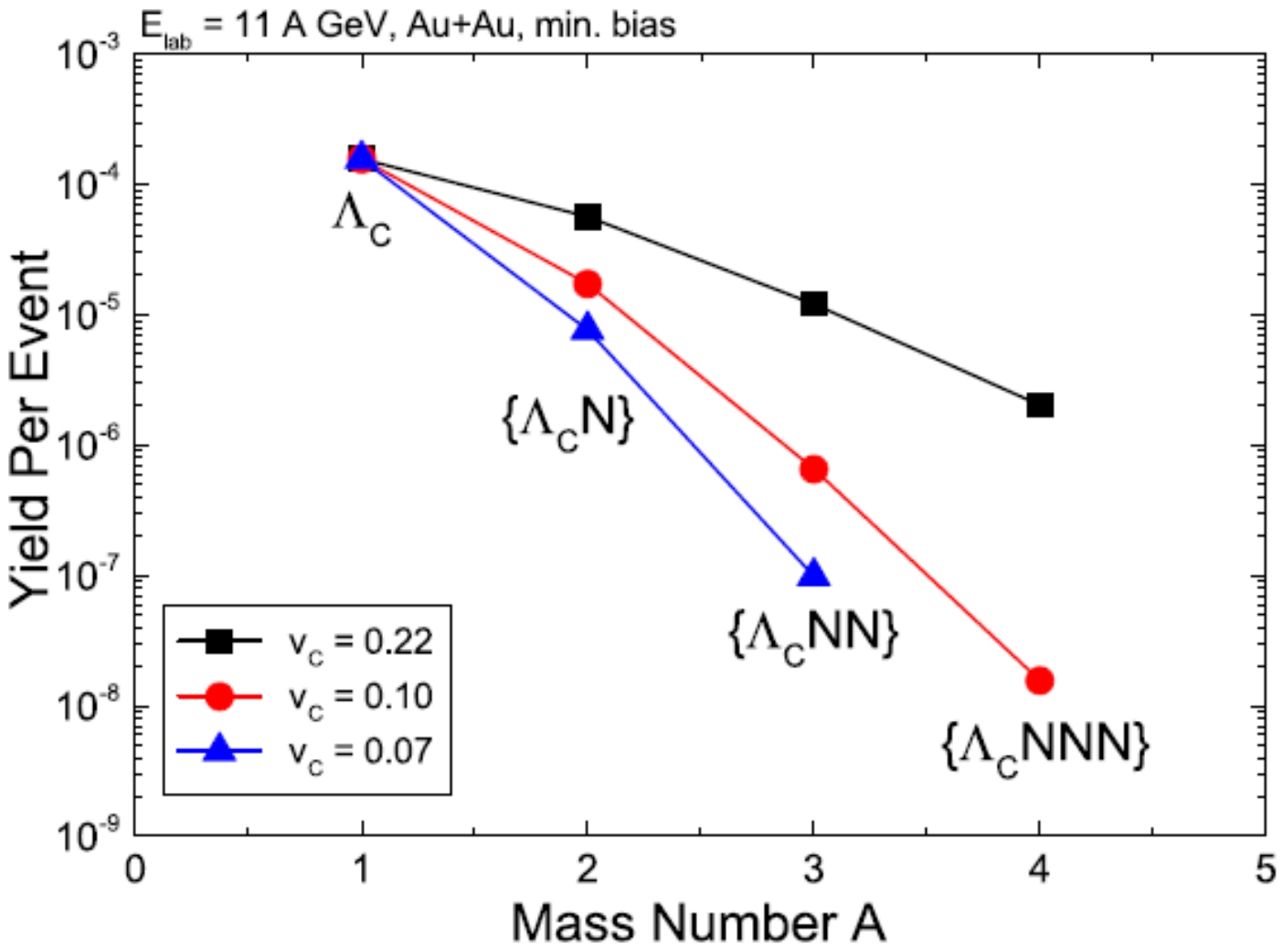

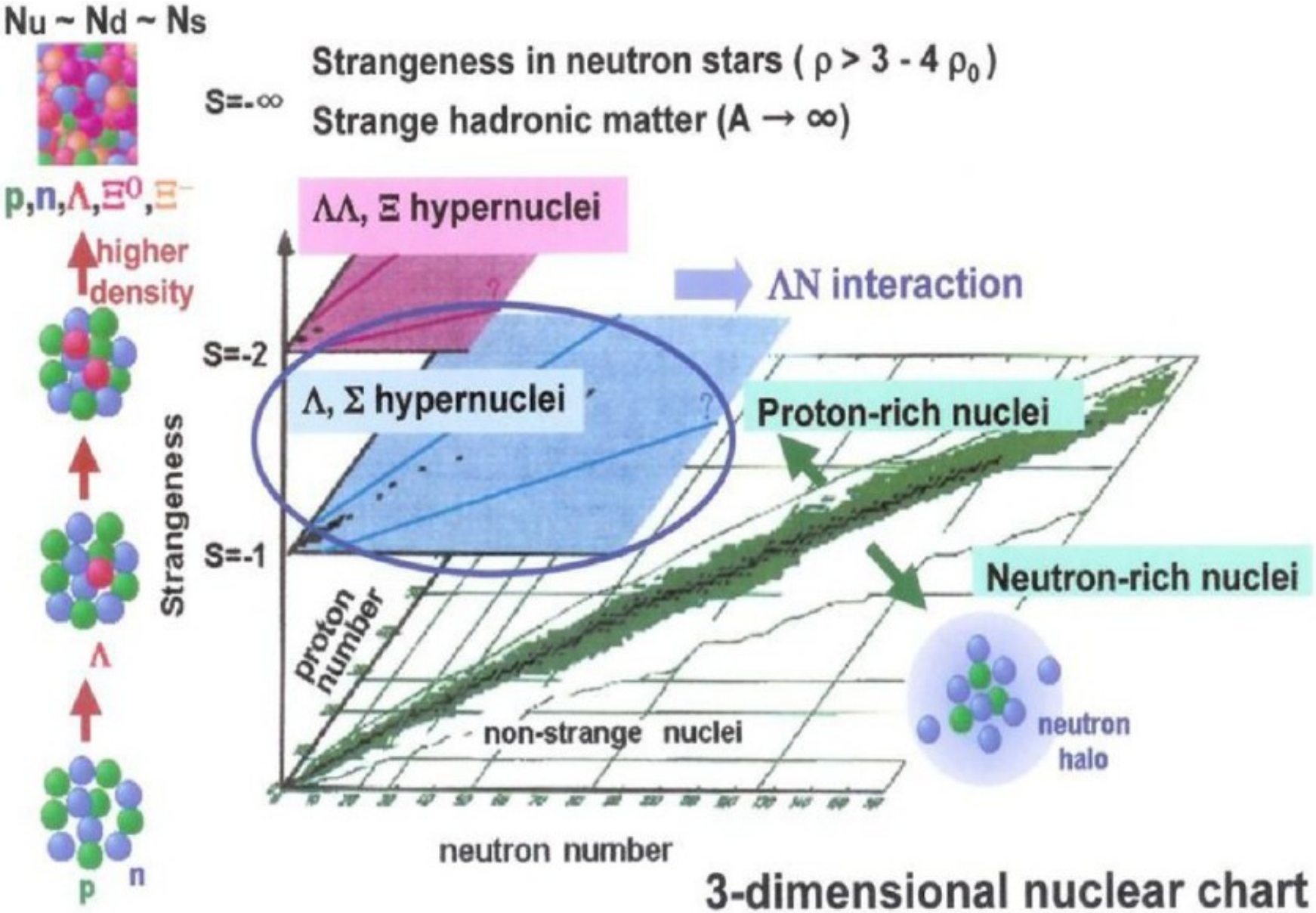
Nu ~ Nd ~ Ns
Strangeness in neutron stars (ρ > 3 - 4 ρ0)
S=-∞
Strange hadronic matter (A → ∞)
p,n,Λ,Ξ0,Ξ−
higher density
ΛΛ, Ξ hypernuclei
ΛN interaction
S=-2
Λ, Σ hypernuclei
Proton-rich nuclei
S=-1
Neutron-rich nuclei
Strangeness
proton number
non-strange nuclei
neutron halo
neutron number
Λ
p
n
3-dimensional nuclear chart

Peripheral collisions. All transport modes predict similar picture: Hyperons can be produced can be produced at all rapidities, in participant and spectator kinematic regions.

Wide rapidity distribution of produced Λ!

Calculation: DCM
PRC**84**(2011)064904

S.Albergo et al.,
E896:
PRL88(2002)062301

Au(11AGeV/c)+Au

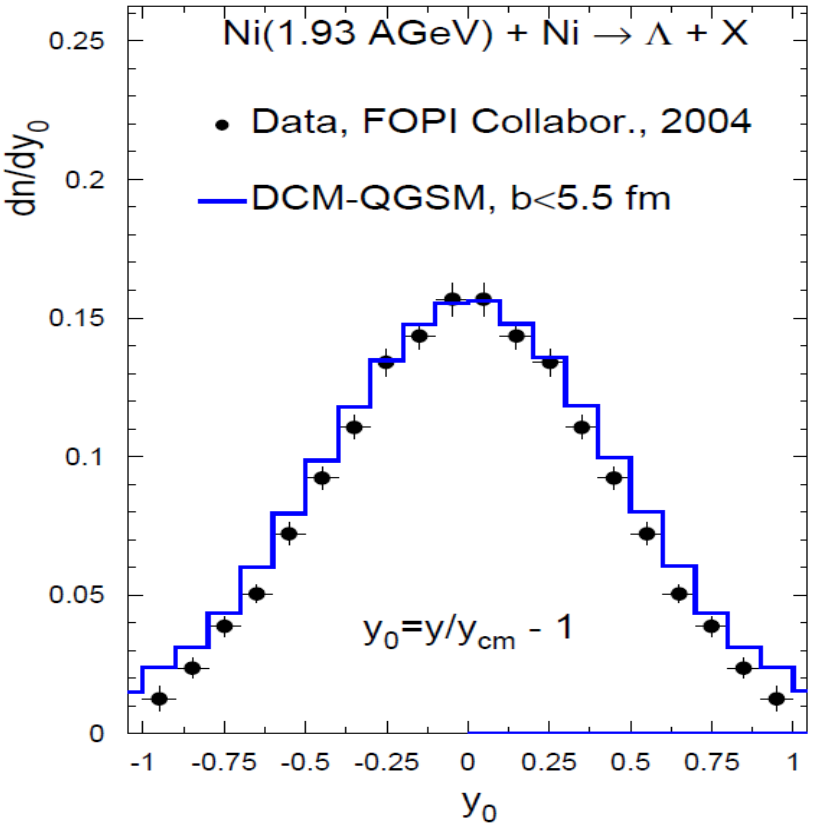

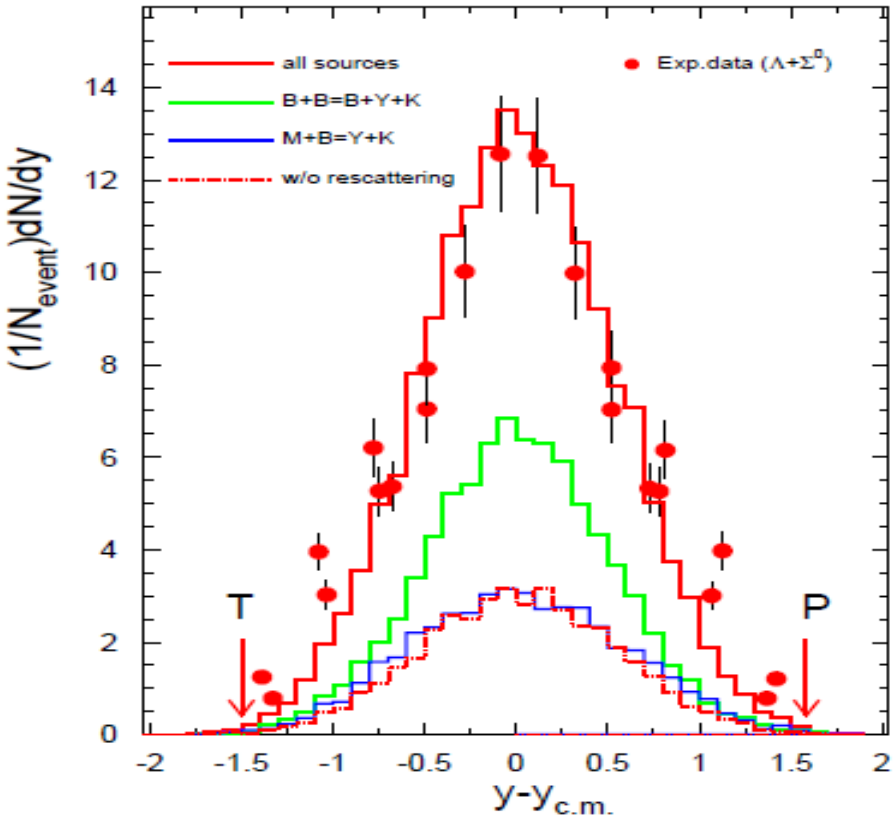

A.Botvina, J.Steinheimer, E.Bratkovskaya, M.Bleicher, J.Pochodzalla, PLB742(2015)7

normal- and hyper-fragments; hyper-residues @ target/projectile rapidities

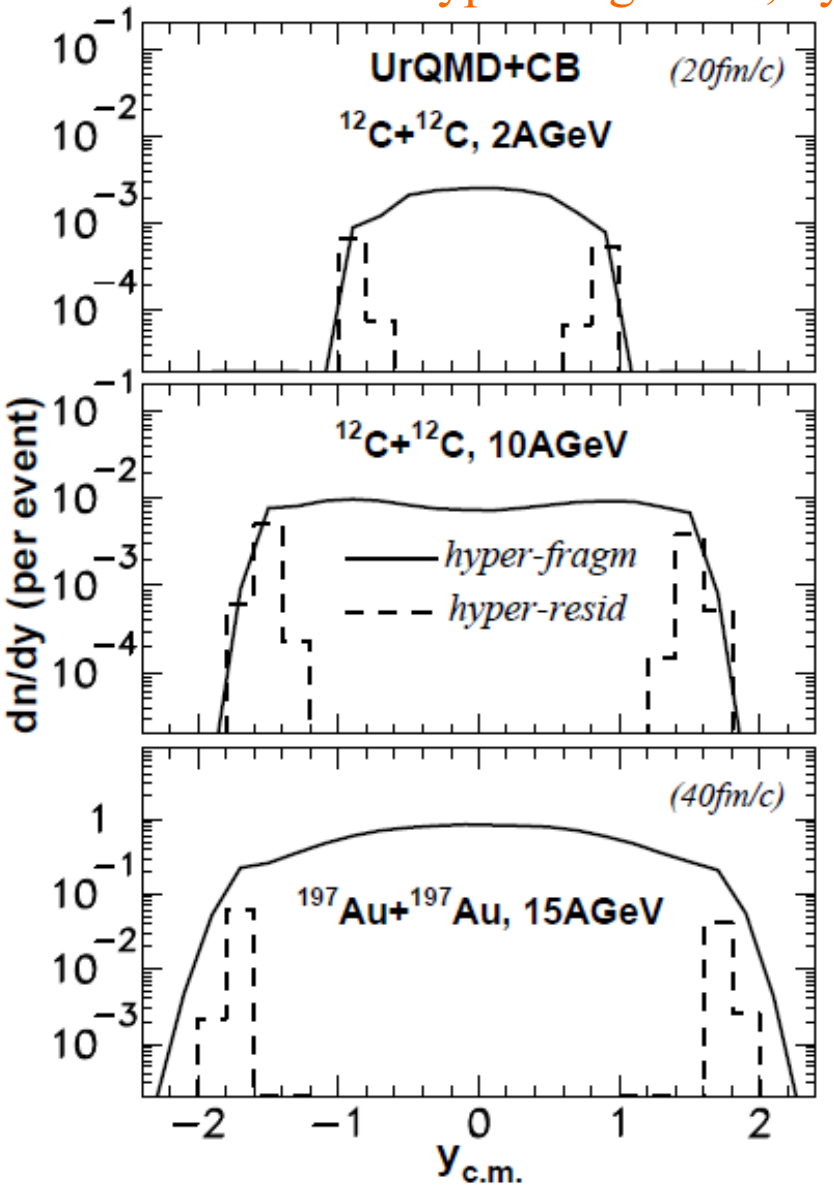

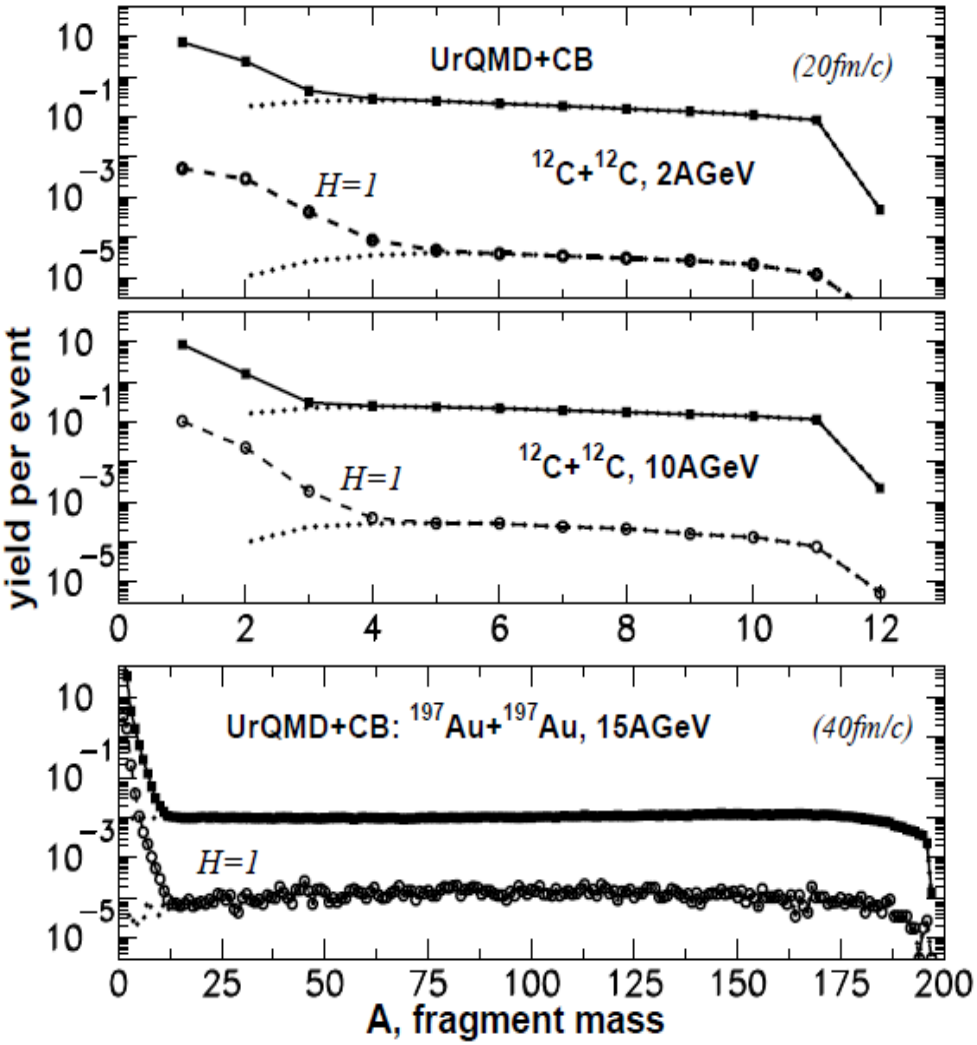

Because of secondary interactions the maximun of the fragments production is shifted from the midrapidity. Secondary products have relatively low kinetic energies, therefore, they can produce clusters and hypernuclei with higher probability.

for LHC @ 2.76 A TeV

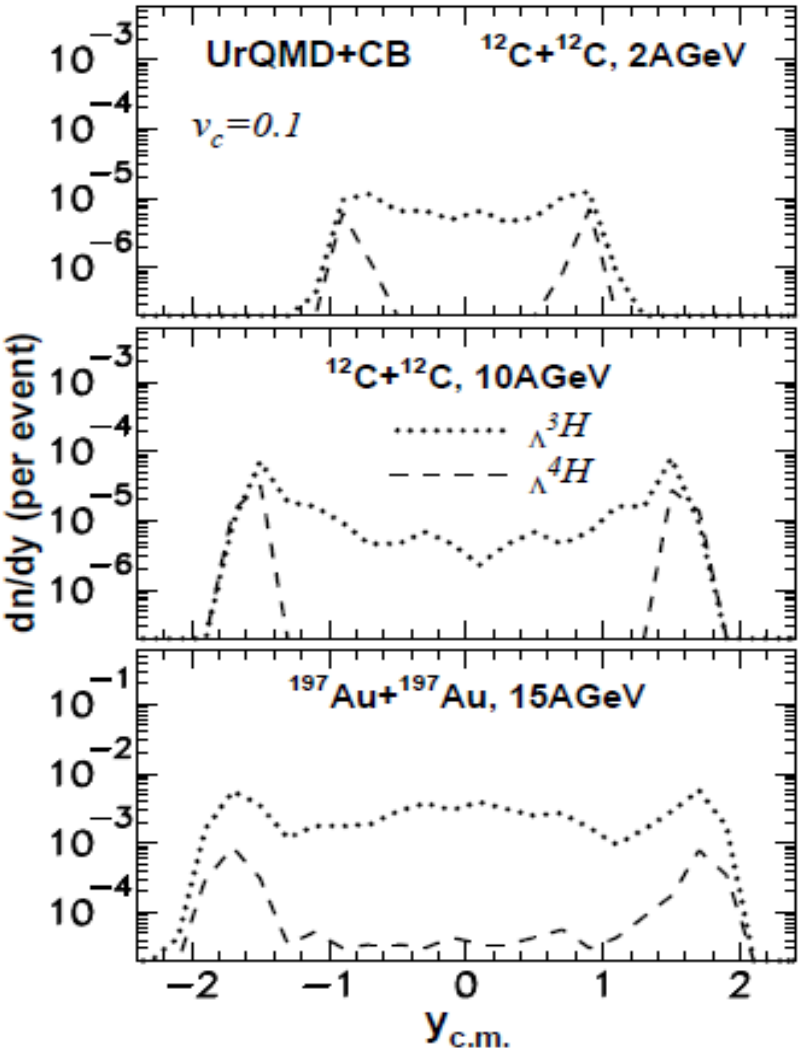

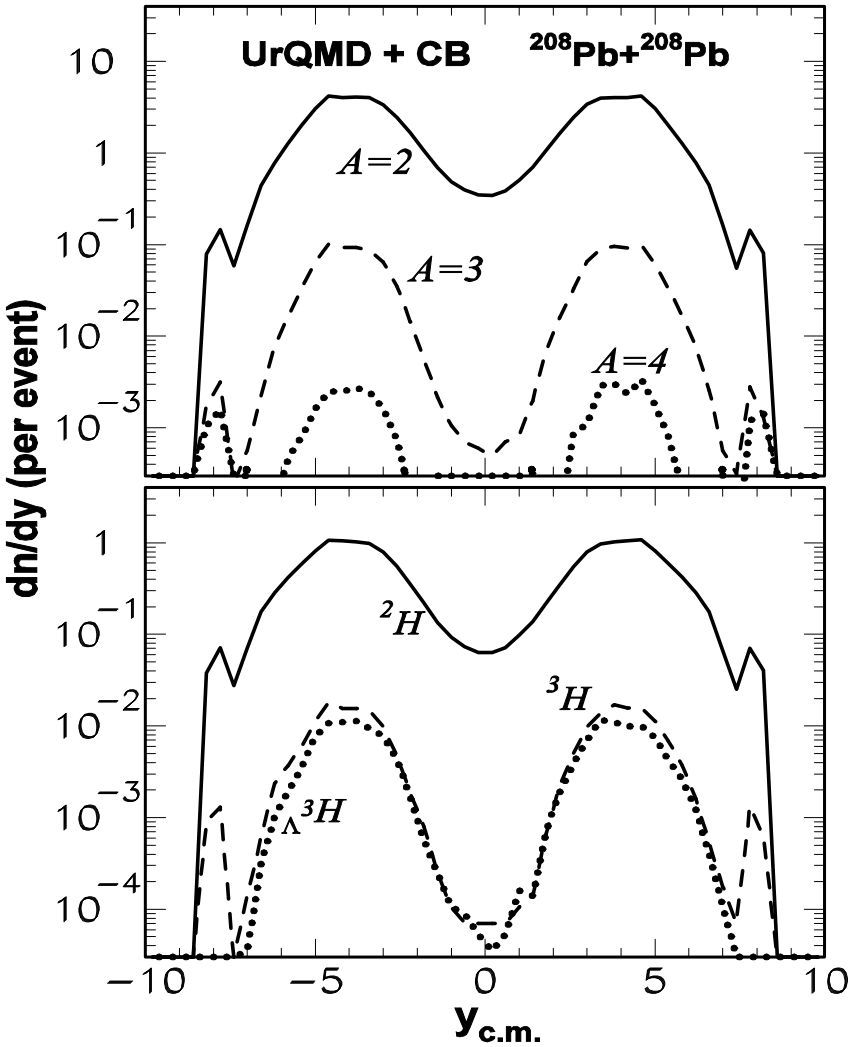

Important features of the fragment formation by the baryon capture in nuclear potential and the coalescence:

Produced fragments are excited, since the capture in ground states has a low probability (suppressed by the phase space). From experiments: there are excited states.

Therefore, the secondary de-excitation is necessary.

Moreover, if we use the statistical approach to describe this de-excitation, a statistical model must be consistent with the initial dynamical description: For example, if we take isospin-depended nuclear potential the de-excitation model must include the isospin dependence in the calculation of the fragment decay (particle emission).

The connection of dynamical and statistical description is a big problem: Sometimes, we may assume that the produced fragments are cold. Simply we select the capture parameters (e.g., coalescence ones) in order to fit measured experimental data.

We must remember that in such a way we can describe only the kinematic characteristics of fragments (e.g., kinetic energies, rapidity distributions), and, roughly, the dependence of their yield vs. mass number. But not their chemical composition.

Novel: coalescent fragments can be excited & undergo de-excitation

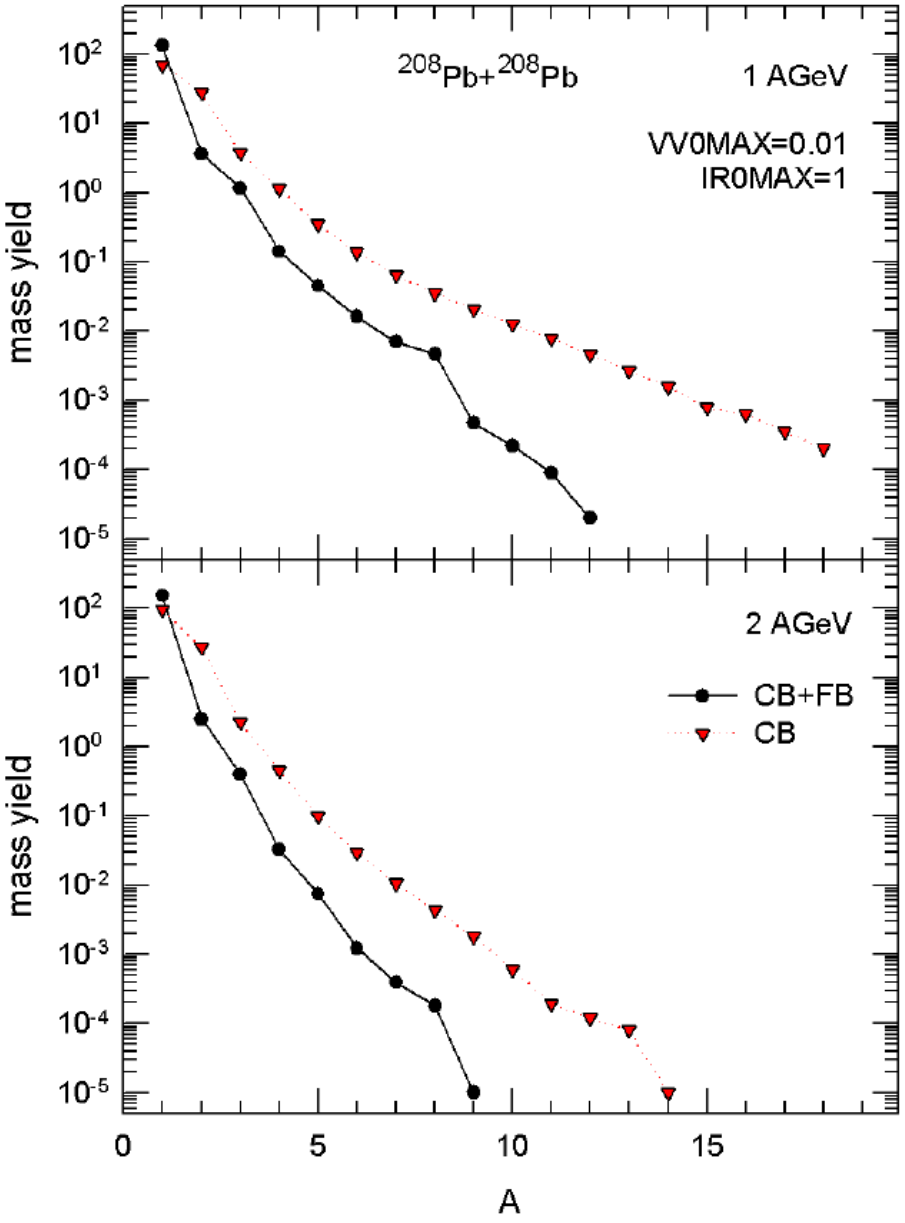

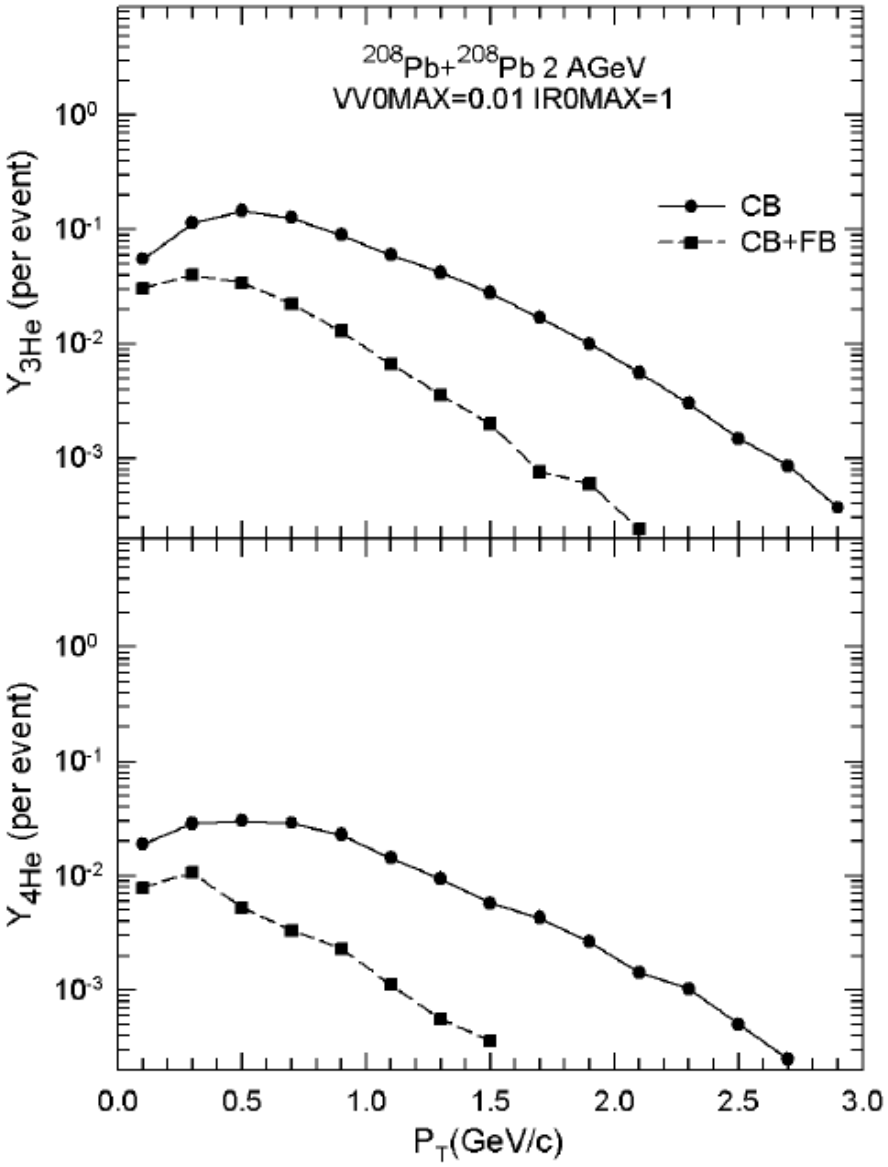

Comparison with experimental data (FOPI/GSI 2010) on light fragment production in central HI collisions. Calculations: Dubna cascade model + coalescence of baryons + statistical multifragmentation model (with evaporartion and Fermi-break-up). Preliminary.

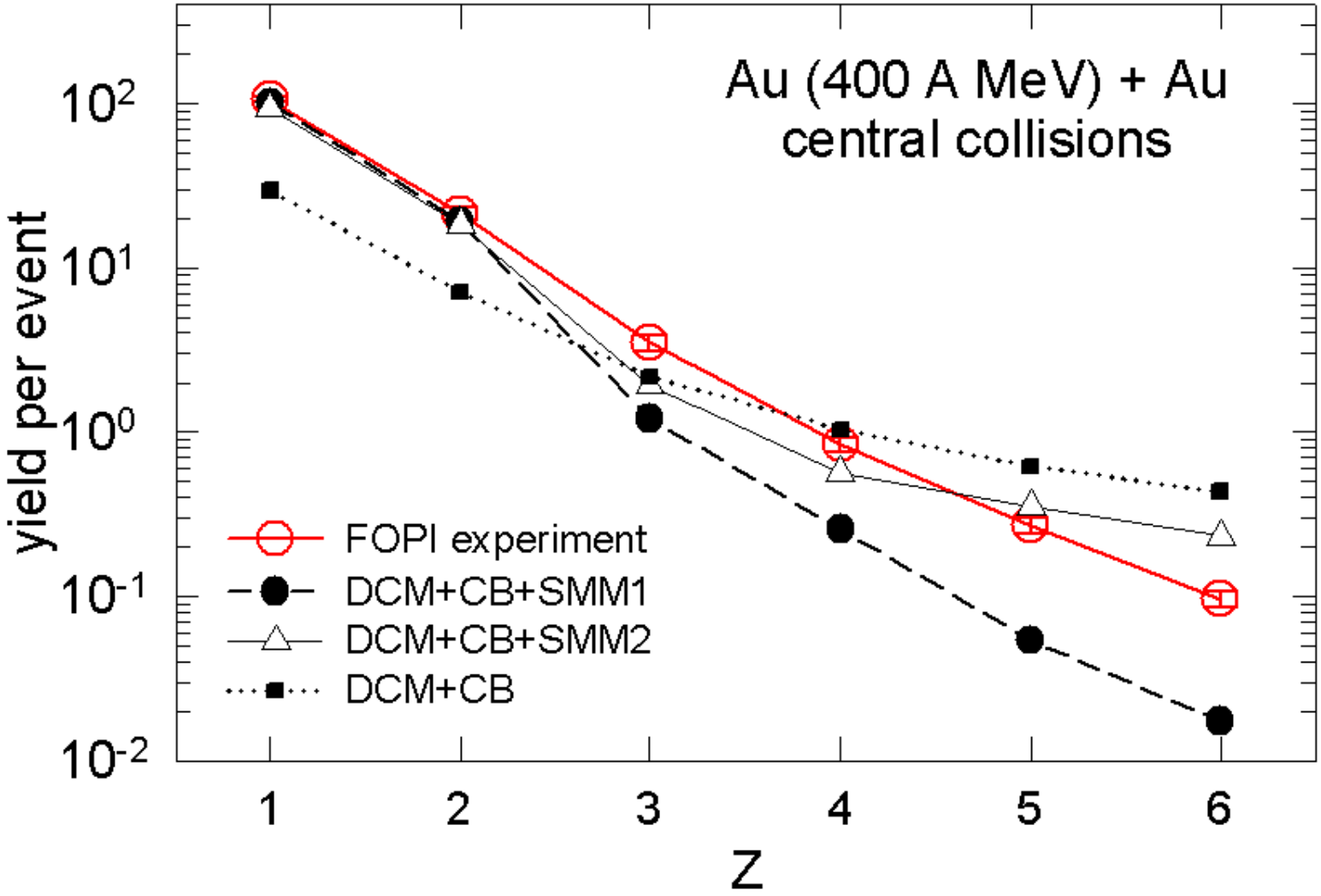

Comparison with FOPI experimental data on 3He and 4He production in central HI collisions. Preliminary.

Yields of these isotopes are modified essentially after the de-excitation processes. The main reason is the binding energy of the fragments inside the freeze-out volume.

Relative behavior of yields of 3He and 4He with energy is important confirmation of the coalescence and statistical mechanisms

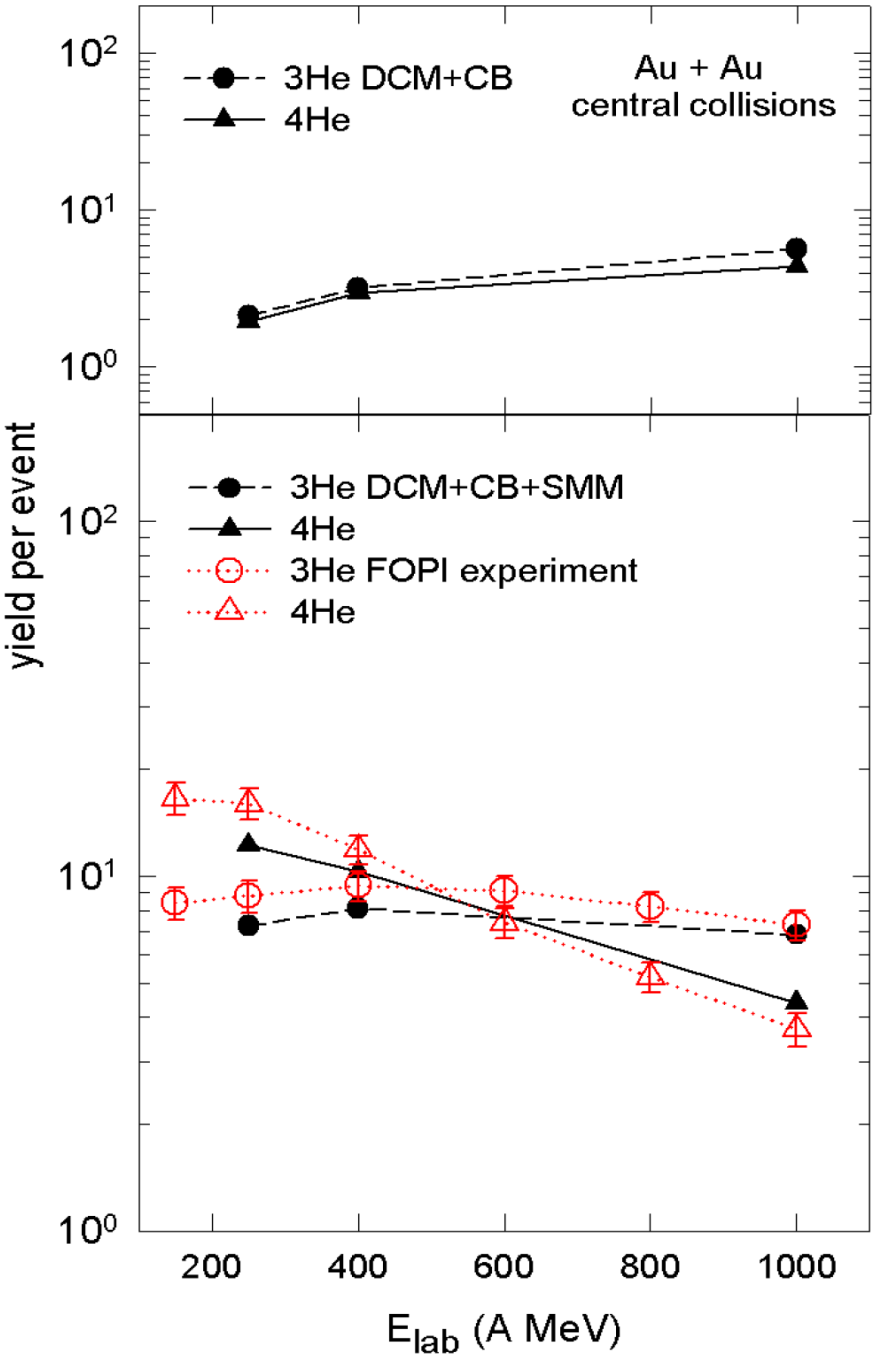

Multifragmentation in intermediate and high energy nuclear reactions

Experimentally established:

1) few stages of reactions leading to multifragmentation,
2) short time ~100fm/c for primary fragment production,
3) freeze-out density is around $0.1\rho_0$,
4) high degree of equilibration at the freeze-out,
5) primary fragments are hot.

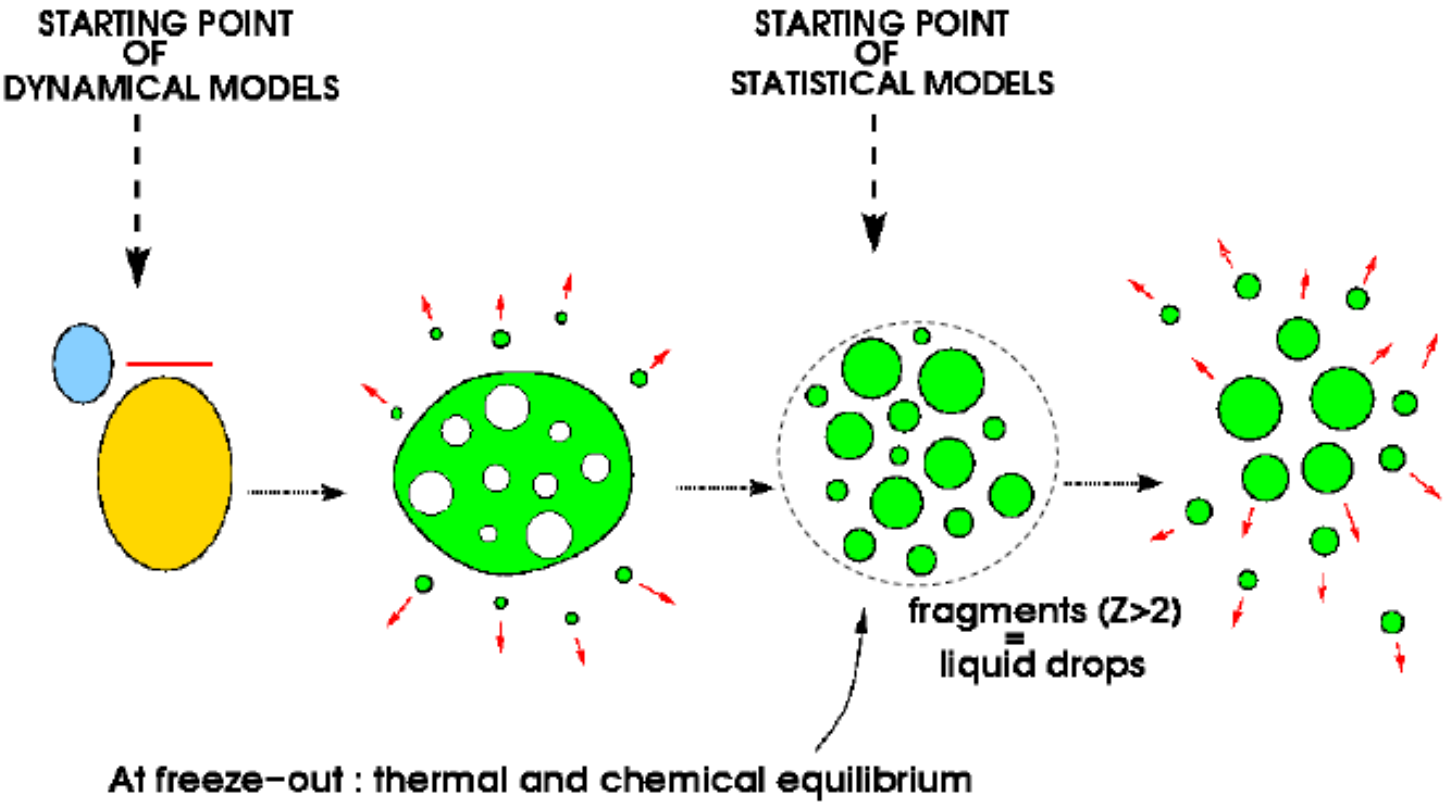

Low/intermediate energies: hadron/lepton collisions with nuclei, the same mechanisms in peripheral relativistic ion collisions

Dinamical stage with particle emission and production of excited nuclear residues

Preequlibrium emission + equilibration

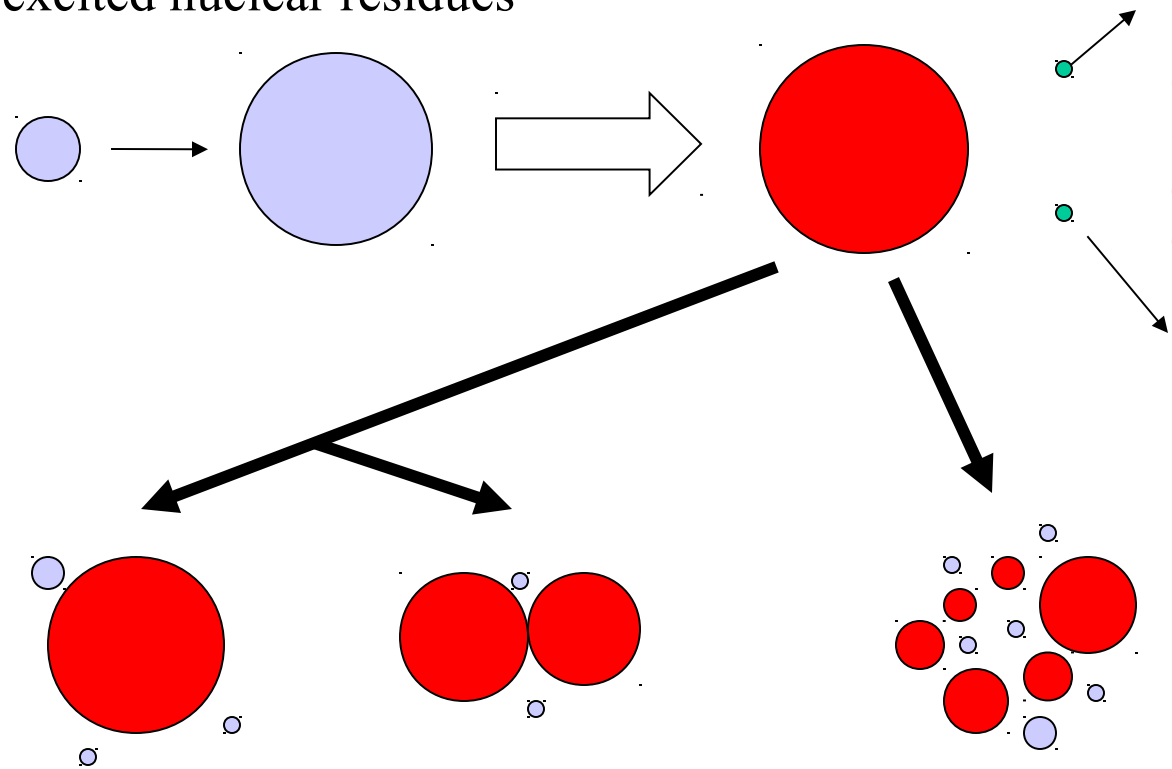

evaporation fission multifragmentation

Statistical approach

N.Bohr (1936)

Compound-nucleus decay channels (sequential evaporation or fission) dominate at low excitation energy of thermal sources E^*<2-3 MeV/nucl

N.Bohr, J.Wheeler (1939)
V.Weisskopf (1937)

starting 1980-th :

At high excitation energy E^*>3-4 MeV/nucl there is a simultaneous break-up into many fragments

Statistical Multifragmentation Model (SMM)

J.P.Bondorf, A.S.Botvina, A.S.Iljinov, I.N.Mishustin, K.Sneppen, Phys. Rep. **257** (1995) 133

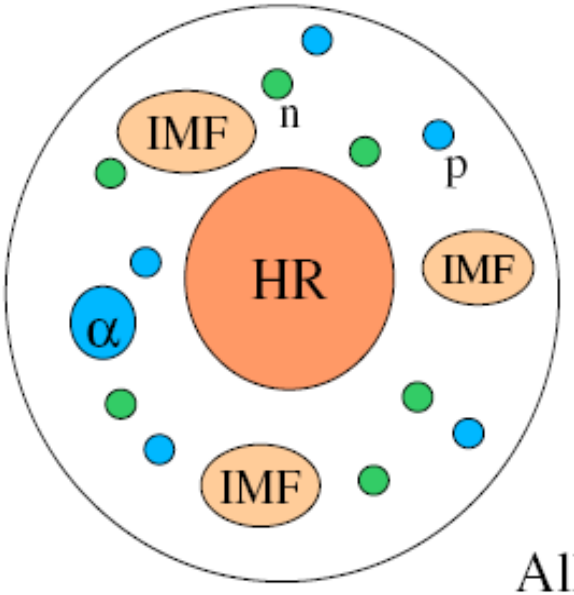

Ensemble of nucleons and fragments
in thermal equilibrium characterized by

neutron number N_0

proton number Z_0, $N_0+Z_0=A_0$

excitation energy $E^*=E_0-E_{CN}$

break-up volume $V=(1+\kappa)V_0$

All break-up channels are enumerated by the sets of fragment multiplicities or partitions, $f=\{N_{AZ}\}$

Statistical distribution of probabilities: $W_f \sim \exp\{S_f(A_0, Z_0, E^*, V)\}$

under conditions of baryon number (A), electric charge (Z) and energy (E*) conservation, including compound nucleus.

Excitation energies of the nuclear spectator residuals

DCM : PRC95, 014902 (2017)

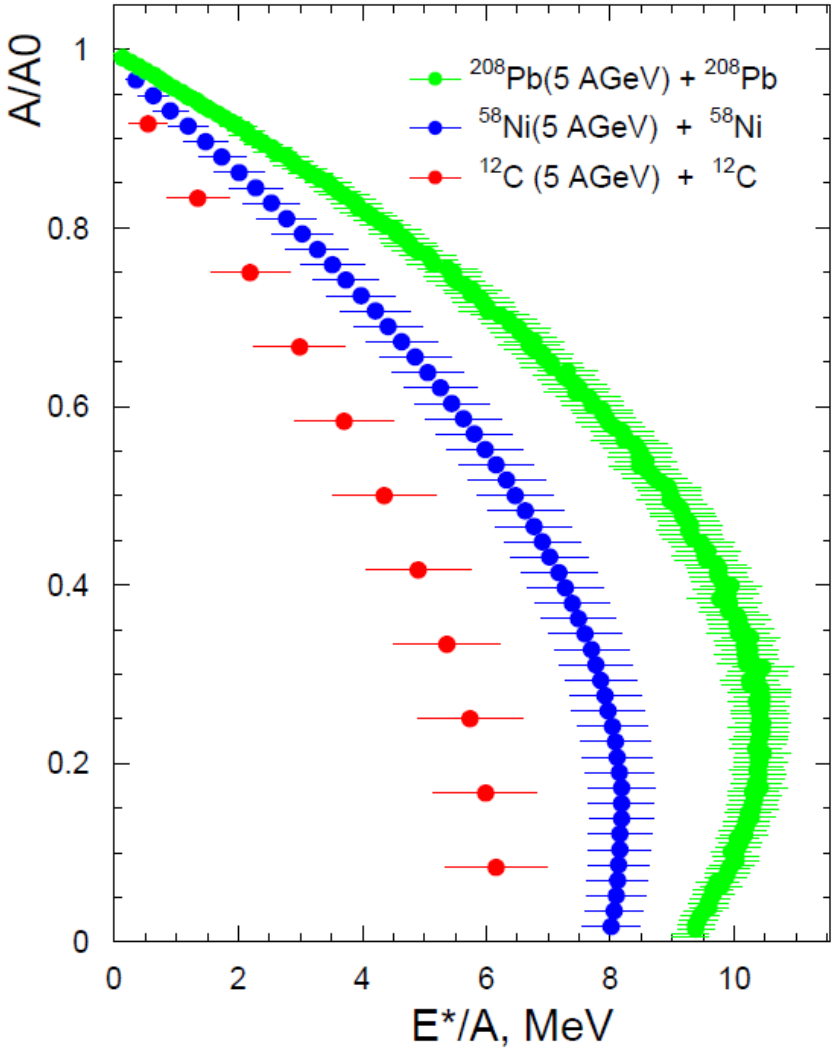

PRC84, 064904 (2011)

Masses of projectile residuals produced at dynamical stage (6b: H=0, 0.2b: H>0)

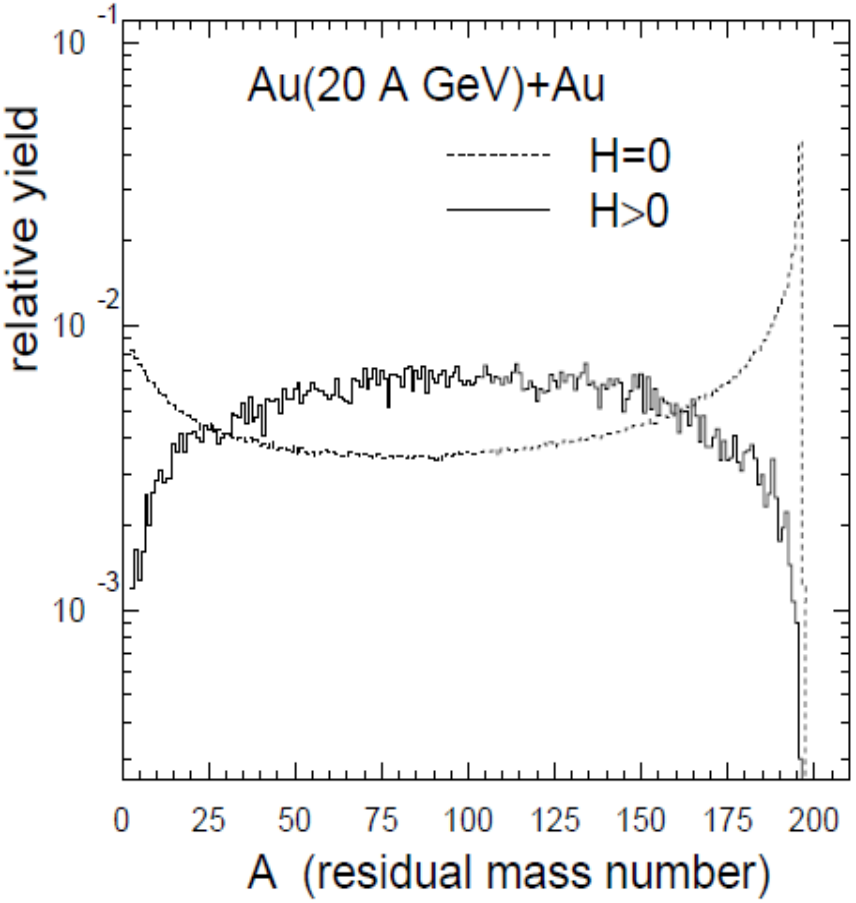

Two-stage multifragmentation of 1*A* GeV Kr, La, and Au

EOS collaboration: fragmentation of relativistic projectiles

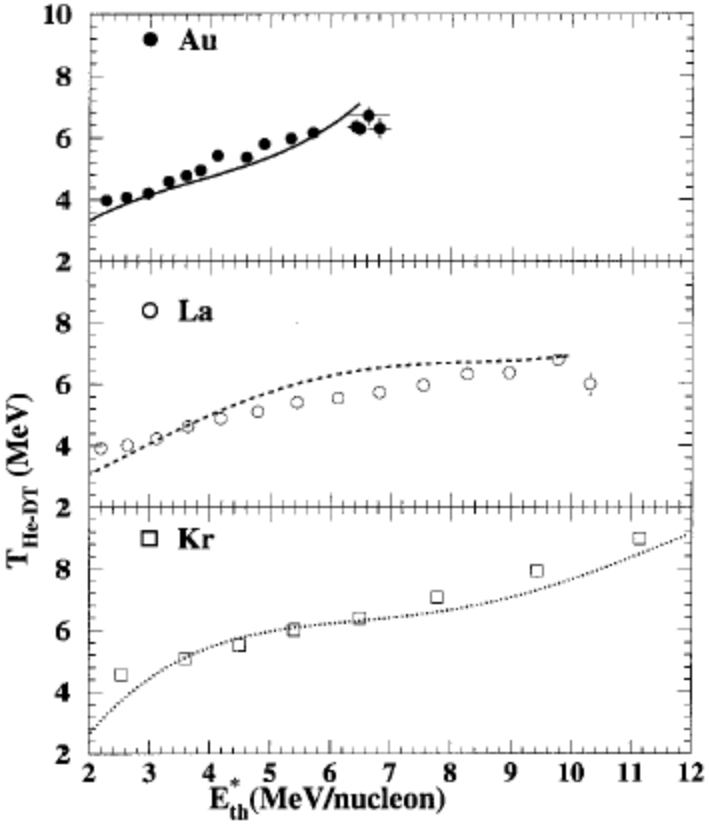

FIG. 19. Caloric curves (T_f vs E^*_{th}/A) for Kr, La, and Au. Points are experimental and curves are from SMM.

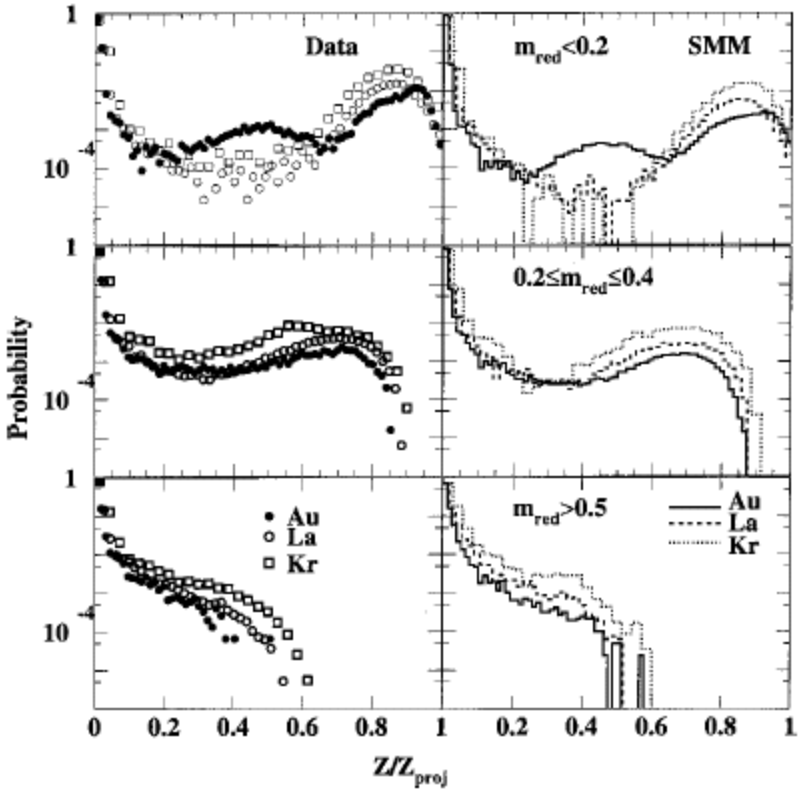

FIG. 24. Second stage fragment charge distribution as a function of $Z/Z_{\text{projectile}}$. Results are shown for three reduced multiplicity intervals for both data and SMM.

ALADIN data

GSI

multifragmentation of relativistic projectiles

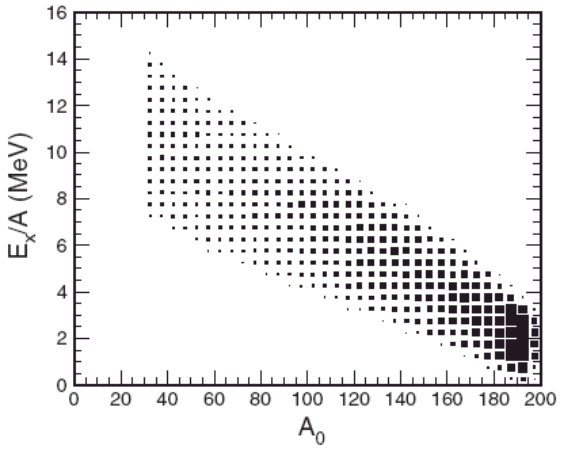

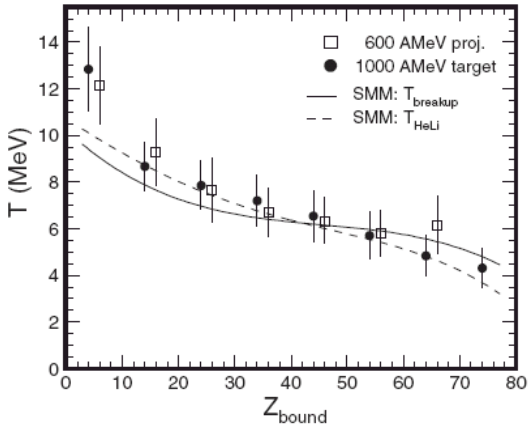

A.S.Botvina et al.,
Nucl.Phys. A584(1995)737

H.Xi et al.,
Z.Phys. A359(1997)397

comparison with SMM (statistical multifragmentation model)

Statistical equilibrium has been reached in these reactions

Au(600MeV/n)+C,Al,Cu

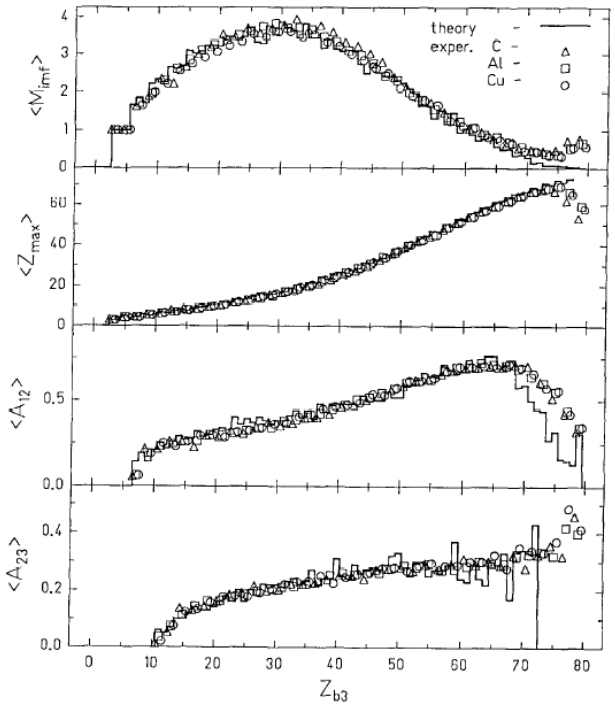

Au(600MeV/n)+Cu

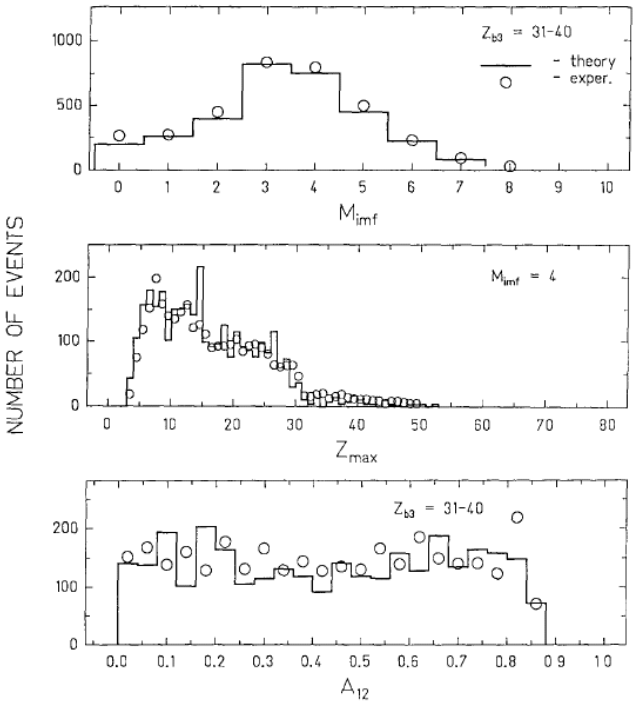

R.Ogul et al. PRC **83,** 024608 (2011) **ALADIN@GSI**

Isospin-dependent multifragmentation of relativistic projectiles

124,107-**Sn**, 124-**La** (600 A MeV) + **Sn** → projectile (multi-)fragmentation

Very good description is obtained within Statistical Multifragmentation Model, including fragment charge yields, isotope yileds, various fragment correlations.

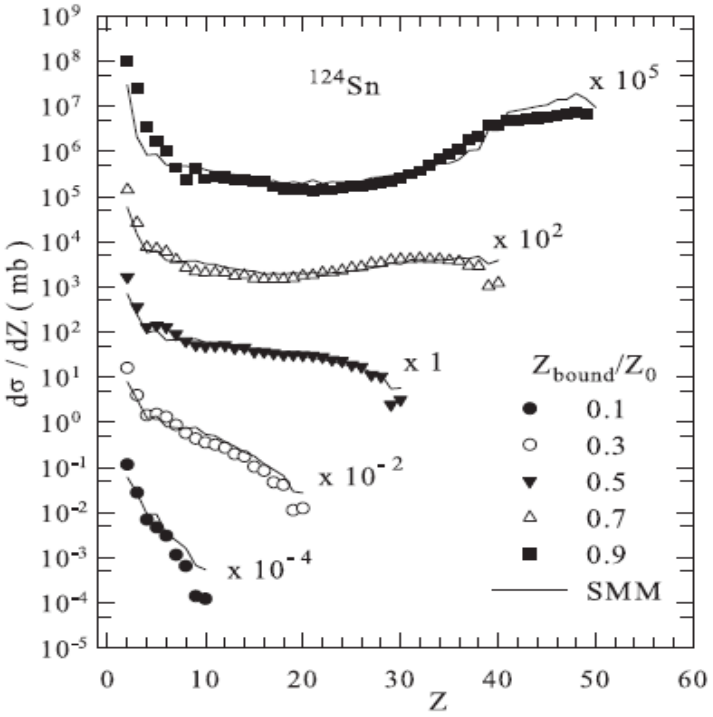

Statistical (chemical) equilibrium is established at break-up of hot projectile residues ! In the case of strangeness admixture we expect it too !

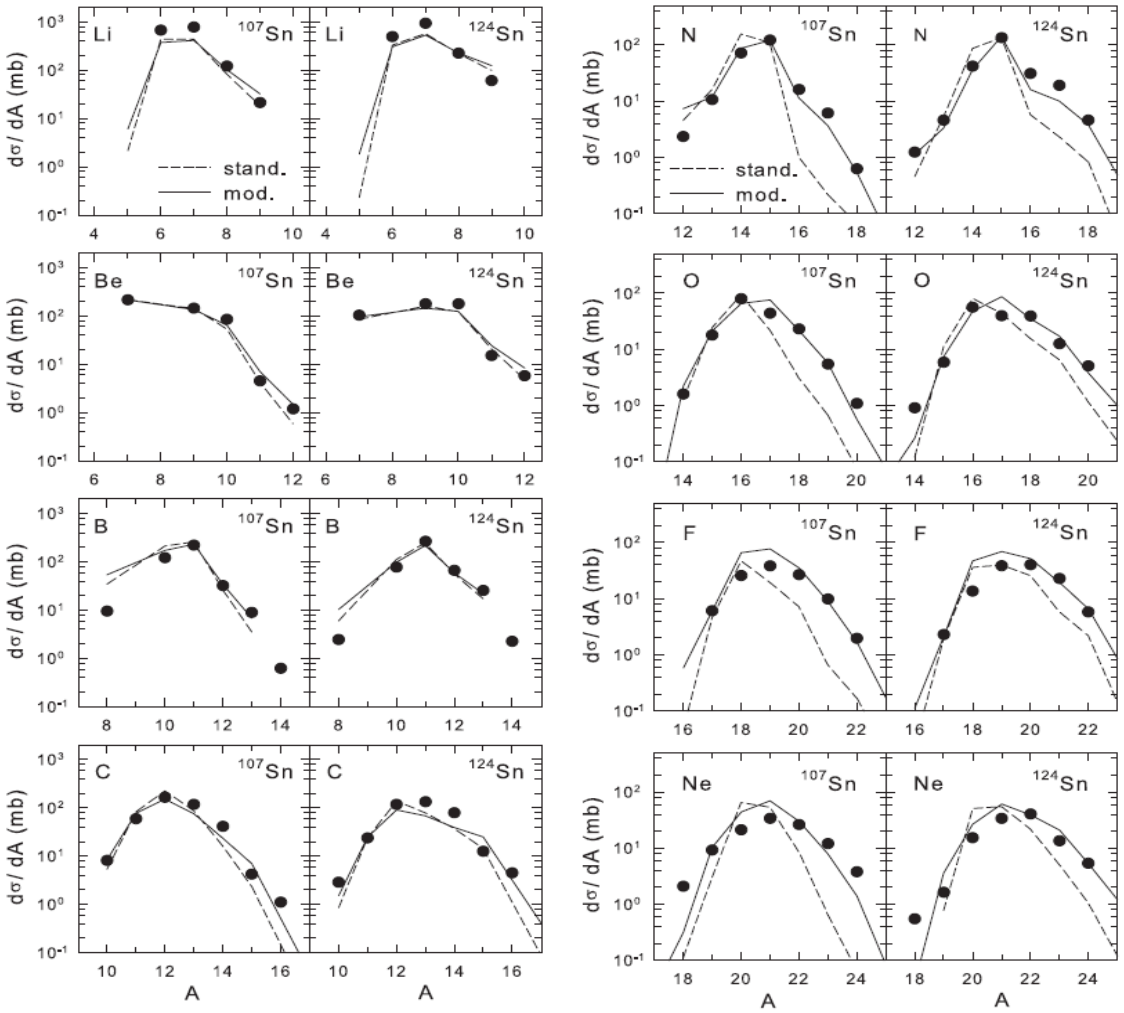

Dynamical+Statistical description of normal multifragmentation

ALADIN data

GSI

multifragmentation of relativistic projectiles

A.S.Botvina et al., Nucl.Phys. A584(1995)737

comparison with SMM (statistical multifragmentation model)

Statistical equilibrium has been reached in these reactions

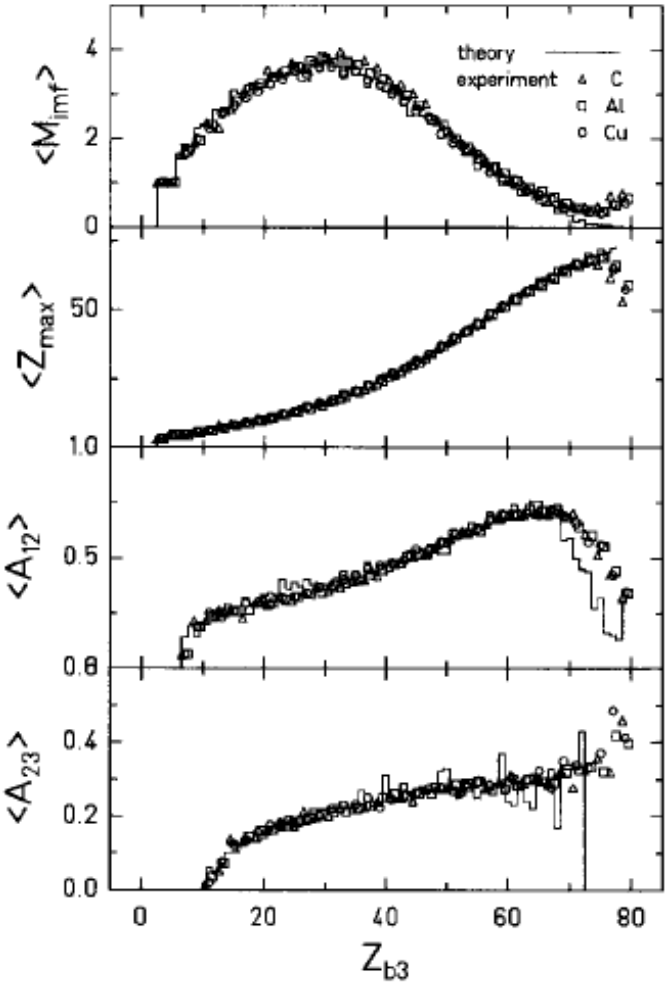

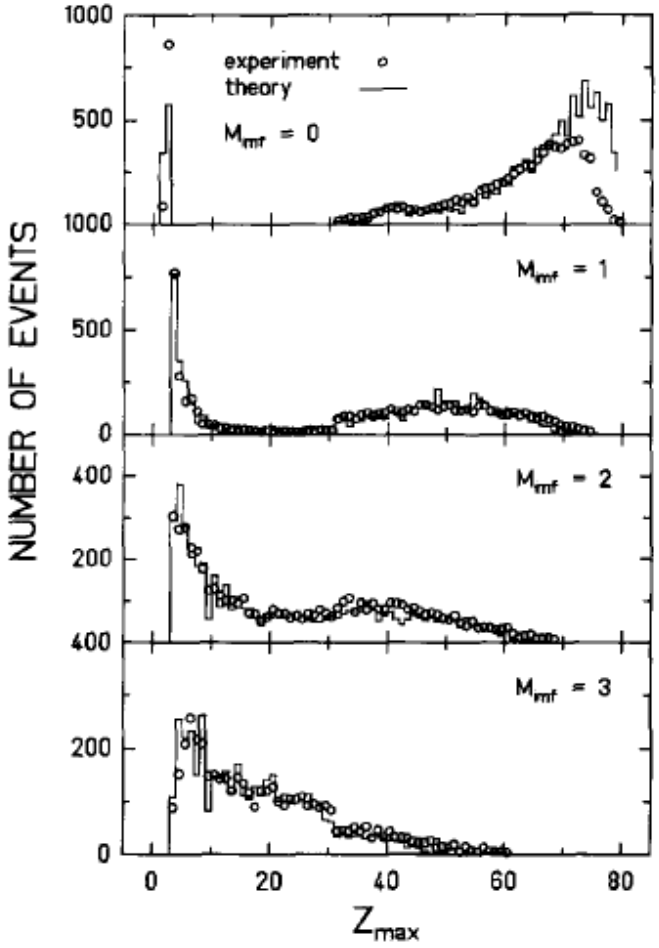

Correlation characteristics are very important for verification of models !

A.S.Botvina and J.Pochodzalla, Phys. Rev.C76 (2007) 024909

Generalization of the statistical de-excitation model for nuclei with Lambda hyperons

In these reactions we expect analogy with

multifragmentation in intermediate and high energy nuclear reactions

+ nuclear matter with strangeness

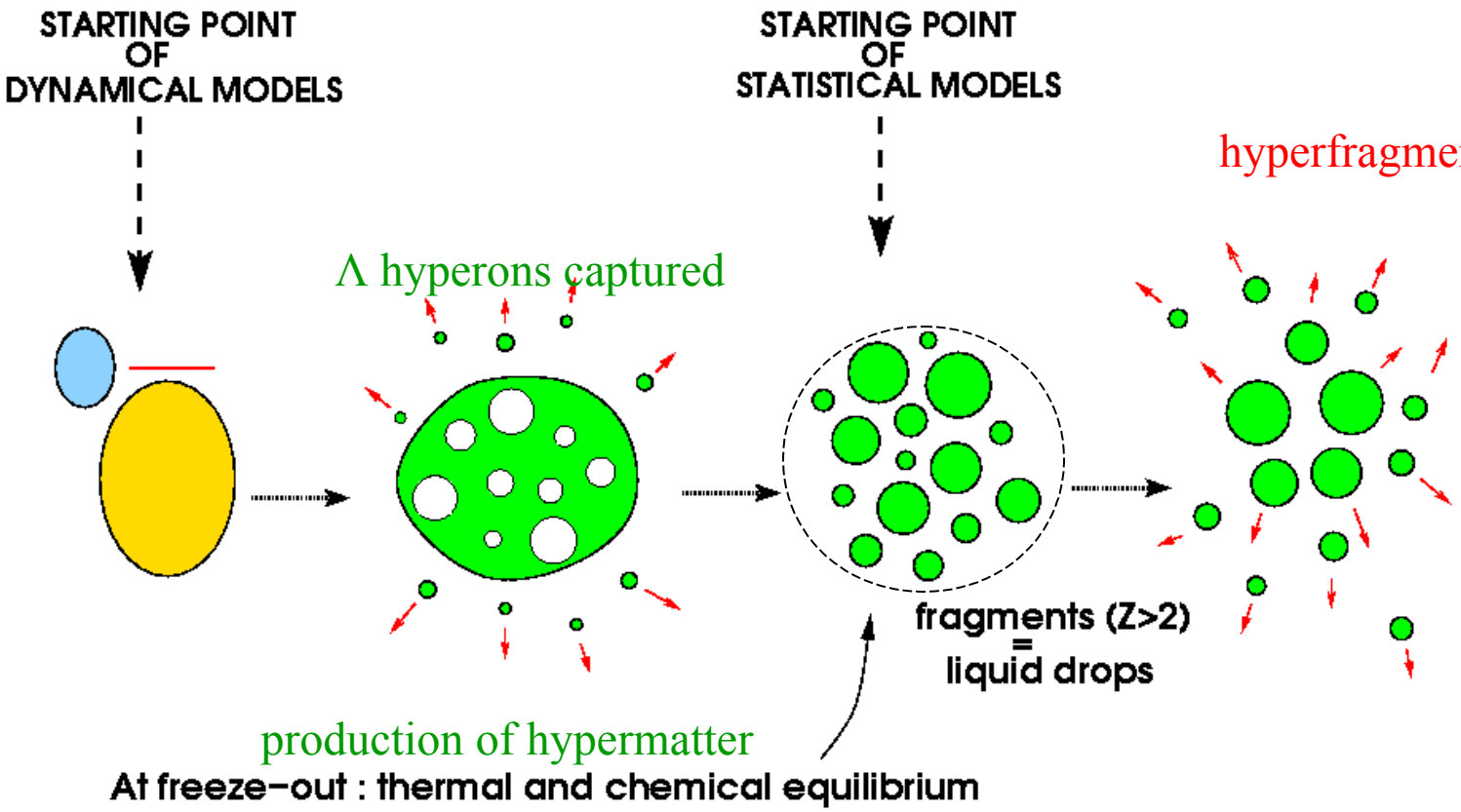

Production of excited hyper-residues in peripheral collisions, decaying into hypernuclei (target/projectile rapidity region).

DCM and UrQMD + CB predictions: Phys. Rev. C95, 014902 (2017)

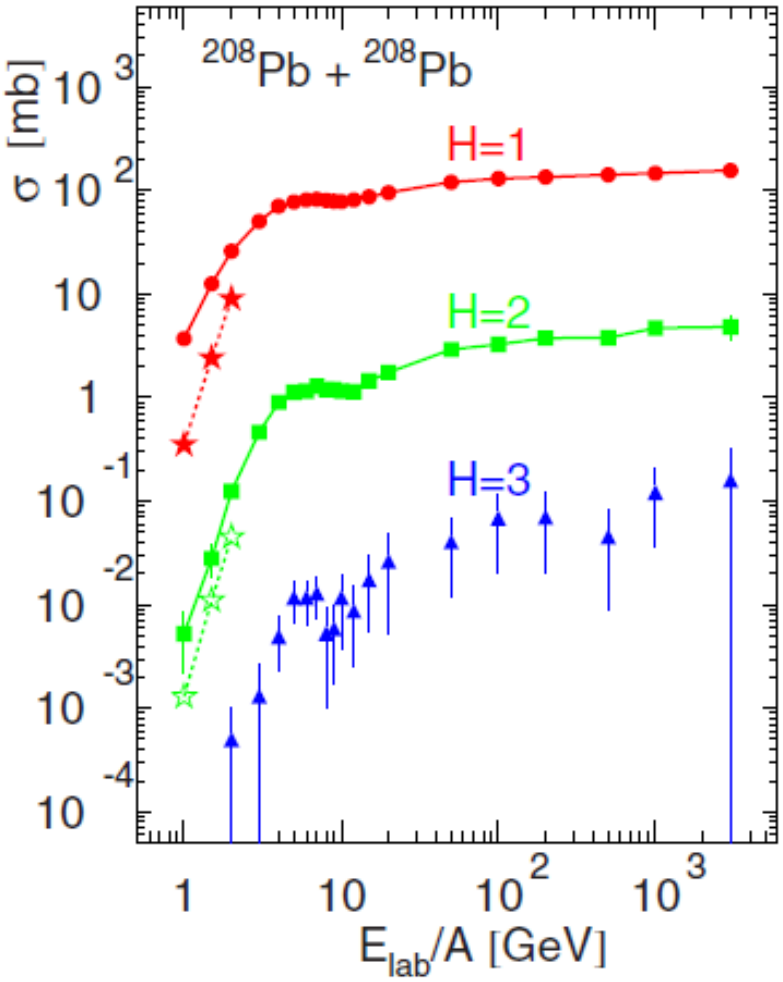

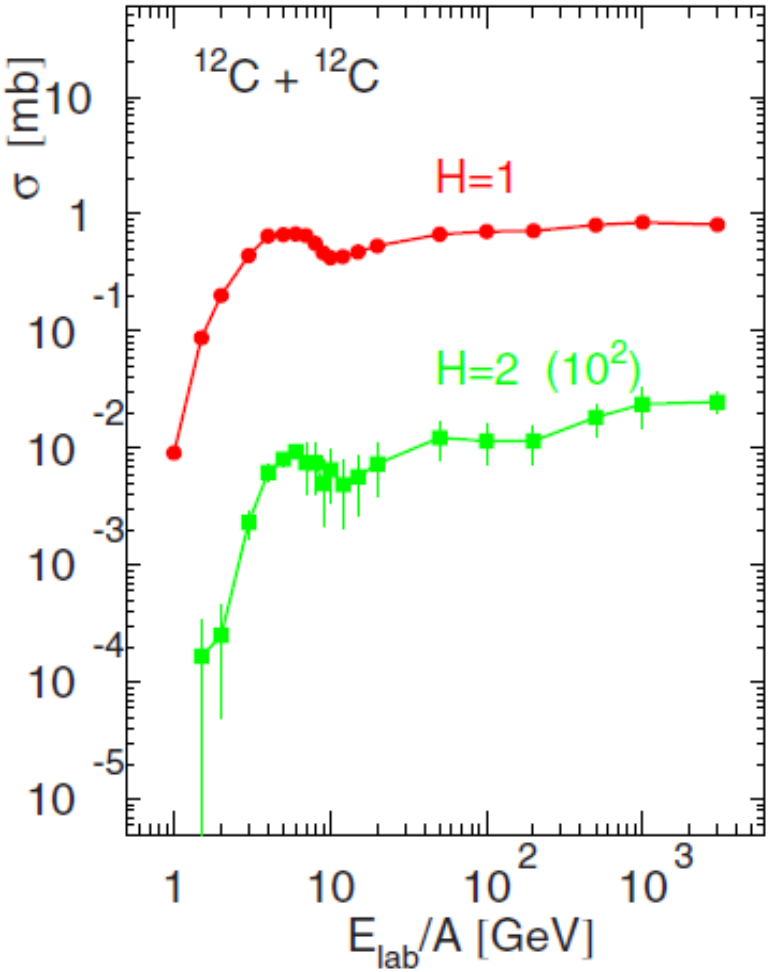

Production of light hypernuclei in relativistic ion collisions

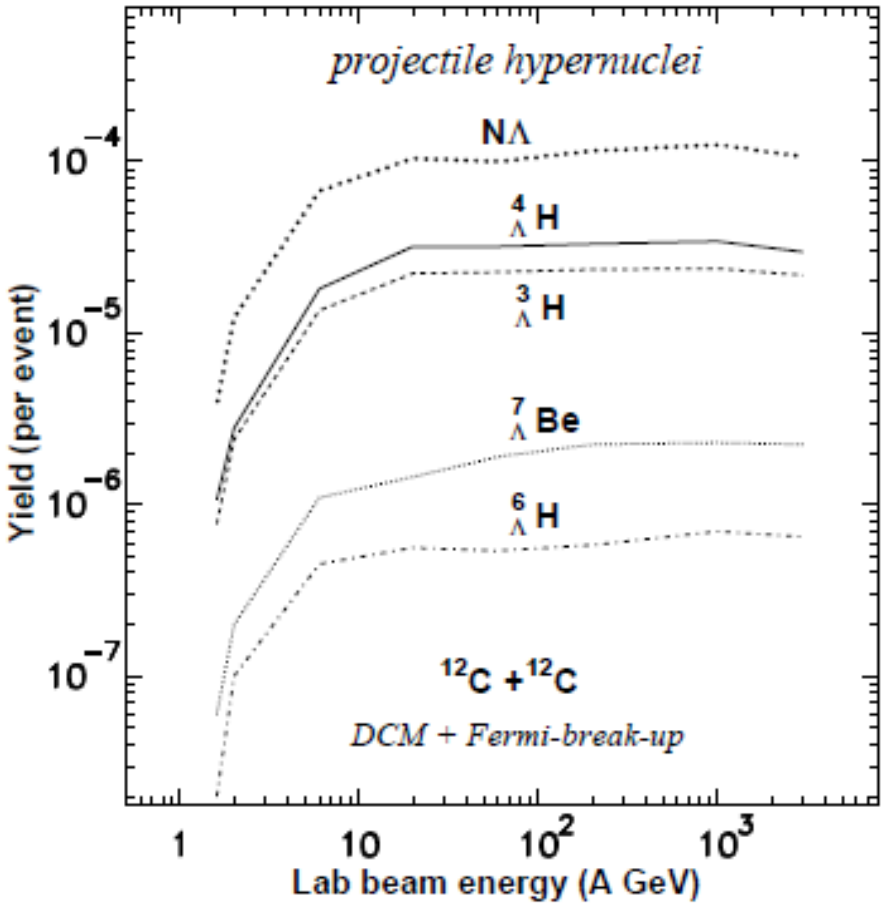

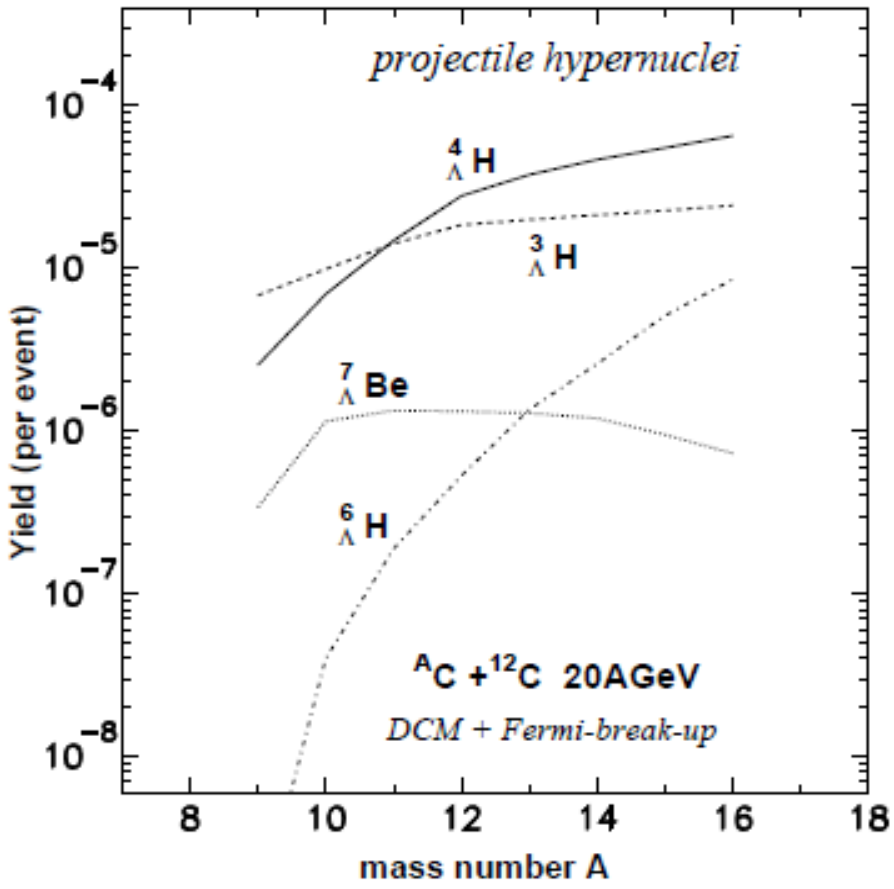

One can use exotic neutron-rich and neutron-poor projectiles, which are not possible to use as targets in traditional hyper-nuclear experiments, because of their short lifetime. Comparing yields of hypernuclei from various sources we can get info about their binding energies and properties of hyper-matter.

A.S.Botvina, K.K.Gudima, J.Pochodzalla, PRC 88, 054605, 2013

Statistical approach for fragmentation of hyper-matter

$$Y_{AZH} = g_{AZH} V_f \frac{A^{3/2}}{\lambda_T^3} \exp\left[-\frac{1}{T}\left(F_{AZH} - \mu_{AZH}\right)\right]$$

$$\mu_{AZH} = A\mu + Z\nu + H\xi$$

mean yield of fragments with mass number A, charge Z, and Λ-hyperon number H

$$F_{AZH}(T,V) = F_A^B + F_A^S + F_{AZH}^{sym} + F_{AZ}^C + F_{AH}^{hyp}$$

liquid-drop description of fragments: bulk, surface, symmetry, Coulomb (as in Wigner-Seitz approximation), and hyper energy contributions
J.Bondorf et al., Phys. Rep. **257** (1995) 133

$$F_A^B(T) = \left(-w_0 - \frac{T^2}{\varepsilon_0}\right) A \quad ,$$

$$F_A^S(T) = \beta_0 \left(\frac{T_c^2 - T^2}{T_c^2 + T^2}\right)^{5/4} A^{2/3} \quad ,$$

parameters ≈ Bethe-Weizsäcker formula:

$w_0 = 16$ MeV, $\beta_0 = 18$ MeV, $T_c = 18$ MeV

$$F_{AZH}^{sym} = \gamma \frac{(A - H - 2Z)^2}{A - H} \quad ,$$

$\gamma = 25$ MeV $\varepsilon_0 \approx 16$ MeV

$$\sum_{AZH} A Y_{AZH} = A_0, \sum_{AZH} Z Y_{AZH} = Z_0, \sum_{AZH} H Y_{AZH} = H_0.$$

chemical potentials are from mass, charge and *H*yperon number conservations

$$F_{AH}^{hyp} = E_{sam}^{hyp} = H \cdot (-10.68 + 48.7/(A^{2/3})).$$

-- C.Samanta et al. J. Phys. G: 32 (2006) 363
(motivated: single Λ in potential well)

$$F_{AH}^{hyp} = (H/A) \cdot (-10.68A + 21.27A^{2/3}).$$

-- liquid-drop description of hyper-matter

A.S.Botvina and J.Pochodzalla, Phys. Rev.C76 (2007) 024909

Abundant hyper-isotope production in multifragmentation (SMM)

Important features of these reactions: wide fragment/isotope distributions

Statistical regularities of fragment production can be employed to learn about fragments!

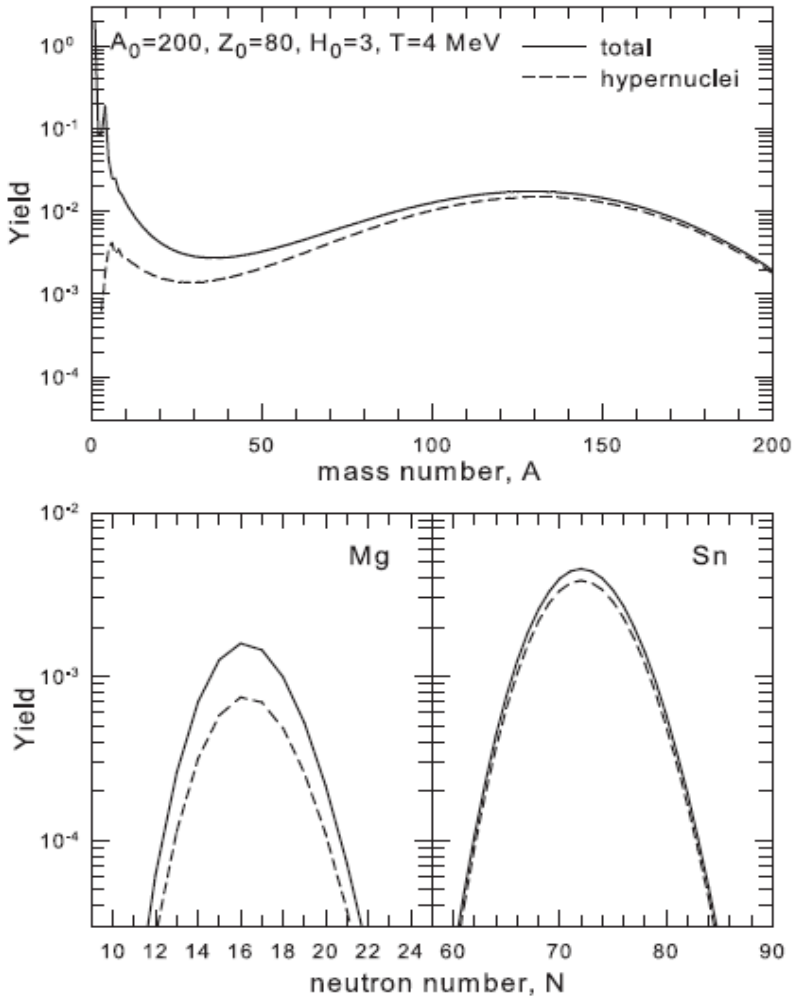

Yields of fragments:

$$Y_{A,Z,H} = g_{A,Z,H} \cdot V_f \frac{A^{3/2}}{\lambda_T^3} \exp\left[-\frac{1}{T}\left(F_{A,Z,H} - \mu_{AZH}\right)\right],$$

$$\mu_{AZH} = A\mu + Z\nu + H\xi.$$

Statistical reaction models can be used not only for the production prediction:

Experimental yields of isotopes can be used for extracting properties of exotic cluster, e.g., the hyperon binding energies

Double ratio method :

ΔE_{bh} **vs** ΔA

difference of hyperon energies in hyper-nuclei: Phys.Rev.C98(2018)064603

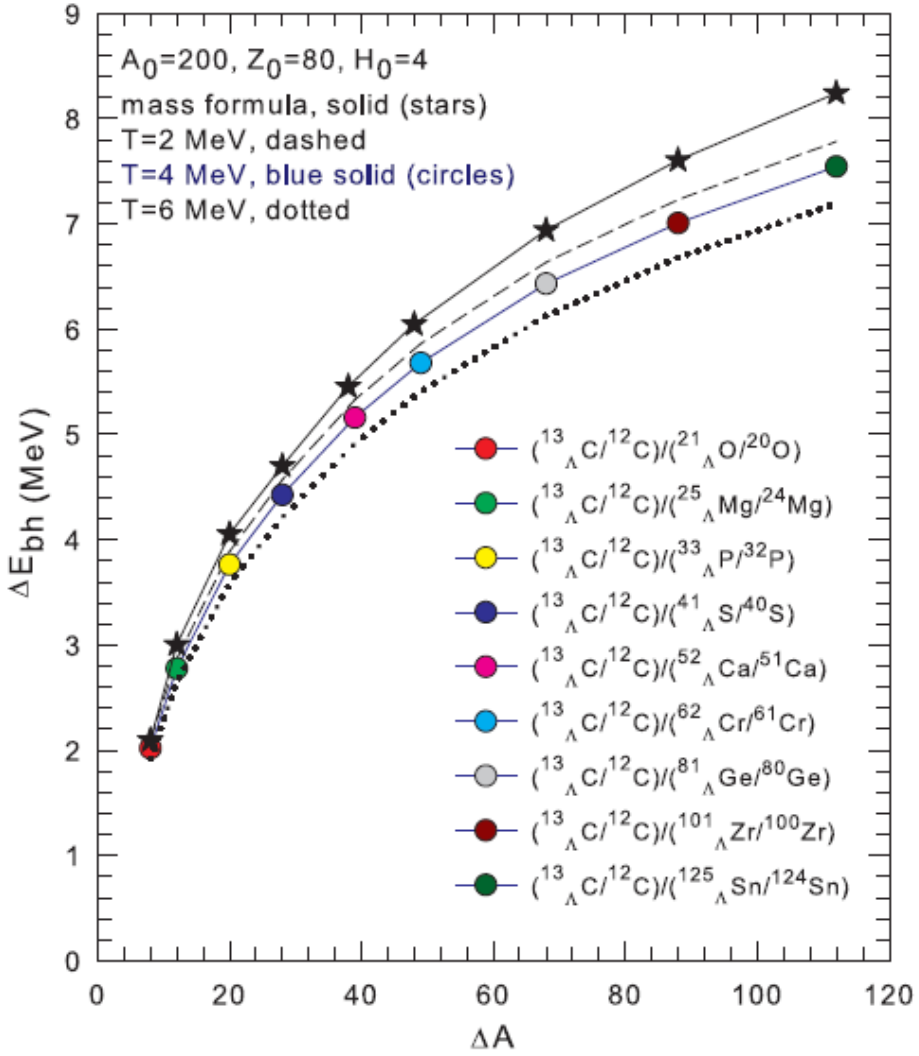

$$\Delta E_{bh} = T \cdot \left[ln\left(\frac{(g_{A_1,Z_1,H}/g_{A_1-1,Z_1,H-1}) \cdot (A_1^{3/2}/(A_1-1)^{3/2})}{(g_{A_2,Z_2,H}/g_{A_2-1,Z_2,H-1}) \cdot (A_2^{3/2}/(A_2-1)^{3/2})}\right) - ln\left(\frac{Y_{A_1,Z_1,H}/Y_{A_1-1,Z_1,H-1}}{Y_{A_2,Z_2,H}/Y_{A_2-1,Z_2,H-1}}\right)\right]$$

Conclusions

Collisions of relativistic ions are promising reactions to search for nuclear clusters, exotic clusters with very different isospin, including hypernuclei. These processes can be simulated within dynamical and statistical models.

Mechanisms of formation of hypernuclei in reactions: Strange baryons (Λ, Σ, Ξ, …) produced in particle collisions can be transported to the spectator residues and captured in nuclear matter. Another mechanism is the coalescence of baryons leading mostly to light clusters will be effective at all rapidities. The produced clusters are presumably excited and after their decay novel hypernuclei of all sizes (and isospin), including short-lived weakly-bound states, multi-strange nuclei can be produced.

Advantages over other reactions: there is no limit on sizes and isotope content of produced exotic nuclei; probability of their formation may be high; a large strangeness can be deposited in nuclei.

Properties of hypernuclei (hyperon binding) can be addressed in novel way!

Correlations (unbound states) and lifetimes can be naturally studied.

EOS and the symmetry energy of hypermatter at subnuclear density and hyperon interactions in exotic nuclear matter can be investigated.

Connection between **coalescence** and **statistical** models
(Eur. Phys. J A17, 559 (2003)):

Coalescence mechanism:

$$\frac{\mathrm{d}^3\langle N_A\rangle}{\mathrm{d}\bar{p}_n^3} \simeq \left(\frac{4\pi}{3}p_0^3\right)^{A-1}\left(\frac{\mathrm{d}^3\langle N_1\rangle}{\mathrm{d}^3\bar{p}_n}\right)^A$$

Assume initial Maxwell-Boltzmann distribution, then

$$\langle N_A\rangle \simeq \left(\frac{4\pi}{3}p_0^3\right)^{A-1}\frac{\langle N_1\rangle^A}{(2\pi m_n T)^{3/2(A-1)}A^{3/2}}.$$

On the other hand, from thermal models one can obtain:

$$\langle N_A\rangle = \langle N_1\rangle^A\left(\frac{\lambda_T^3}{V}\right)^{A-1}A^{3/2}\exp\left(-\frac{B_A}{T_A}\right)$$

We get connection between coalescence parameter and fragment binding energy

$$\frac{4\pi p_0^3 V}{3h^3} \simeq \left(A^3\cdot\exp\left(-\frac{B_A}{T_A}\right)\right)^{1/(A-1)}$$

FOPI data: fragment production in central HI collisions

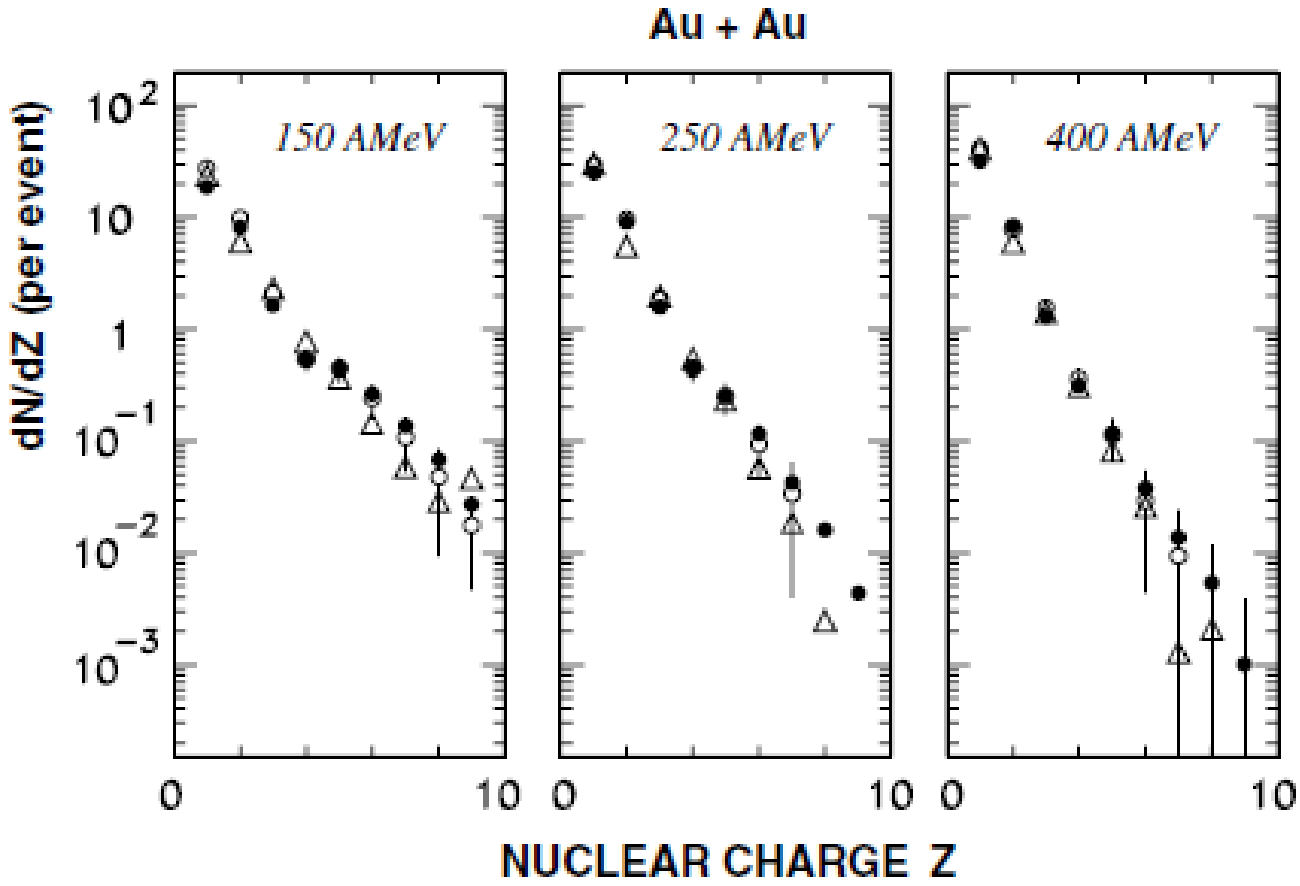

Both coalescence and statistical descriptions are possible - EPJ A 17, 559 (2003). However, the statistical model requires flow and decreasing the source size with energy.

Discovery of a Strange nucleus: Hypernucleus

M. Danysz and J. Pniewski, Philos. Mag. 44 (1953) 348

First-hypernucleus was observed in a stack of photographic emulsions exposed to cosmic rays at about 26 km above the ground.

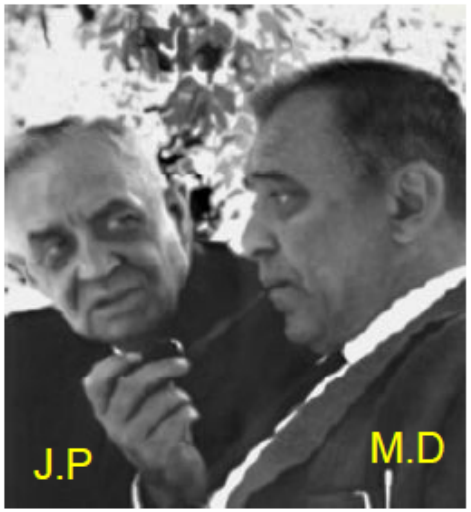

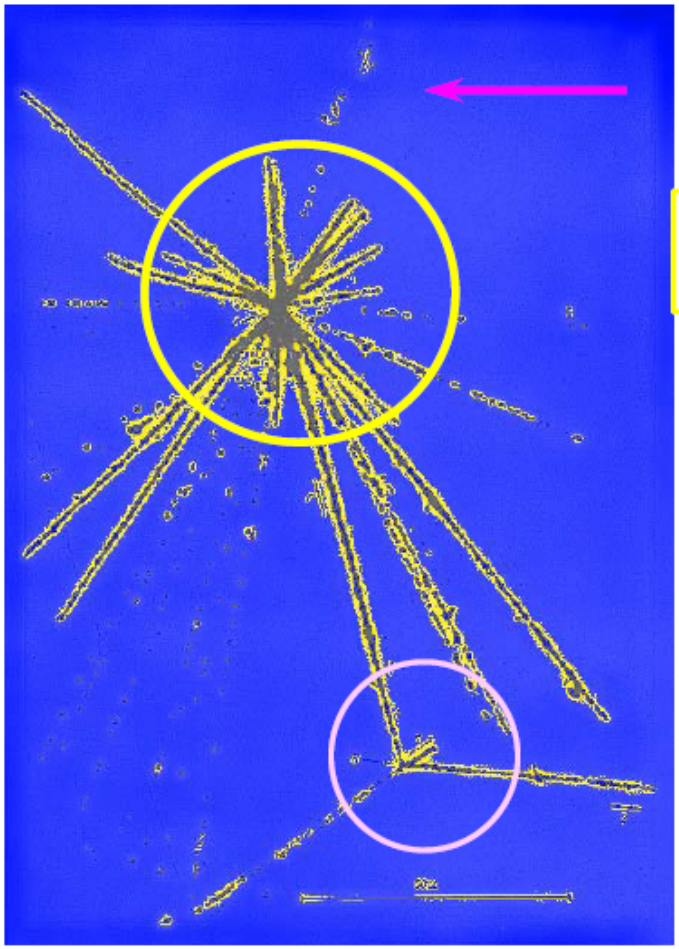

Incoming high energy proton from cosmic ray

colliding with a nucleus of the emulsion, breaks it in several fragments forming a star. **Multifragmentation !**

All nuclear fragments stop in the emulsion after a short path

From the first star, 21 Tracks => $9\alpha + 11H + 1\ {}_{\Lambda}X$

The fragment ${}_{\Lambda}X$ disintegrates later , makes the bottom star. Time taken ~ 10^{-12} sec (typical for weak decay)

This particular nuclear fragment, and the others obtained afterwards in similar conditions, were called **hyperfragments or hypernuclei.**

4.3.3. Evaporation from hot fragments

The successive particle emission from hot primary fragments with $A > 16$ is assumed to be their basic de-excitation mechanism. Due to the high excitation energy of these fragments, the standard Weisskopf evaporation scheme [2] was modified to take into account the heavier ejectiles up to ^{18}O, besides light particles (nucleons, d, t, α), in ground and particle-stable excited states [81]. This corresponds to the excitation energies $\epsilon^{(i)}$ of the ejectiles not higher than 7–8 MeV. By analogy with standard model the width for the emission of a particle j from the compound nucleus (A, Z) is given by:

$$\Gamma_j = \sum_{i=1}^{n} \int_0^{E^*_{AZ} - B_j - \epsilon_j^{(i)}} \frac{\mu_j g_j^{(i)}}{\pi^2 \hbar^3} \sigma_j(E) \frac{\rho_{A'Z'}(E^*_{AZ} - B_j - E)}{\rho_{AZ}(E^*_{AZ})} E\, dE \tag{60}$$

Here the sum is taken over the ground and all particle-stable excited states $\epsilon_j^{(i)} (i = 0, 1, \ldots, n)$ of the fragment j, $g_j^{(i)} = (2s_j^{(i)} + 1)$ is the spin degeneracy factor of the ith excited state, μ_j and B_j are corresponding reduced mass and separation energy, E^*_{AZ} is the excitation energy of the initial nucleus (55), E is the kinetic energy of an emitted particle in the centre-of-mass frame. In Eq. (60) ρ_{AZ} and $\rho_{A'Z'}$ are the level densities of the initial (A, Z) and final (A', Z') compound nuclei. They are calculated using the Fermi-gas formula (41). The cross section $\sigma_j(E)$ of the inverse reaction $(A', Z') + j = (A, Z)$ was calculated using the optical model with nucleus–nucleus potential from Ref. [117]. The evaporational process was simulated by the Monte Carlo method using the algorithm described in Ref. [118]. The conservation of energy and momentum was strictly controlled in each emission step.

Evaporation from hypernuclei: nucleons, light particles, hyperons, light hypernuclei: New masses and assuming the level densities as in normal nuclei.

4.3.4. Nuclear fission

An important channel of de-excitation of heavy nuclei ($A > 200$) is fission. This process competes with particle emission. Following the Bohr–Wheeler statistical approach we assume that the partial width for the compound nucleus fission is proportional to the level density at the saddle point $\rho_{sp}(E)$ [1]:

$$\Gamma_f = \frac{1}{2\pi\rho_{AZ}(E^*_{AZ})} \int_0^{E^*_{AZ}-B_f} \rho_{sp}(E^*_{AZ} - B_f - E)\, dE, \tag{61}$$

where B_f is the height of the fission barrier which is determined by the Myers–Swiatecki prescription [120]. For approximation of ρ_{sp} we used the results of the extensive analysis of nuclear fissility and Γ_n/Γ_f branching ratios [121]. The influence of the shell structure on the level densities ρ_{sp} and ρ_{AZ} is disregarded since in the case of multifragmentation we are dealing with very high excitation energies $E^* > 30$–50 MeV when shell effects are expected to be washed out [122].

Fission of hypernuclei: New fission barriers including hyperon interaction (in the liquid-drop approach). It leads to increasing the barriers for ~ 1 MeV.
The level densities at the saddle point are taken as in normal nuclei (first approximation).

Evaporation & Fission of hypernuclei

(depending on mass and excitation energy)

A.S.Botvina et al., Phys. Rev. C94 (2016) 054615

These processes recall normal fission and evaporation. However, producing exotic hyper-fragments is possible (e.g. neutron rich ones) to investigate hyperon interactions in astro-physical conditions.

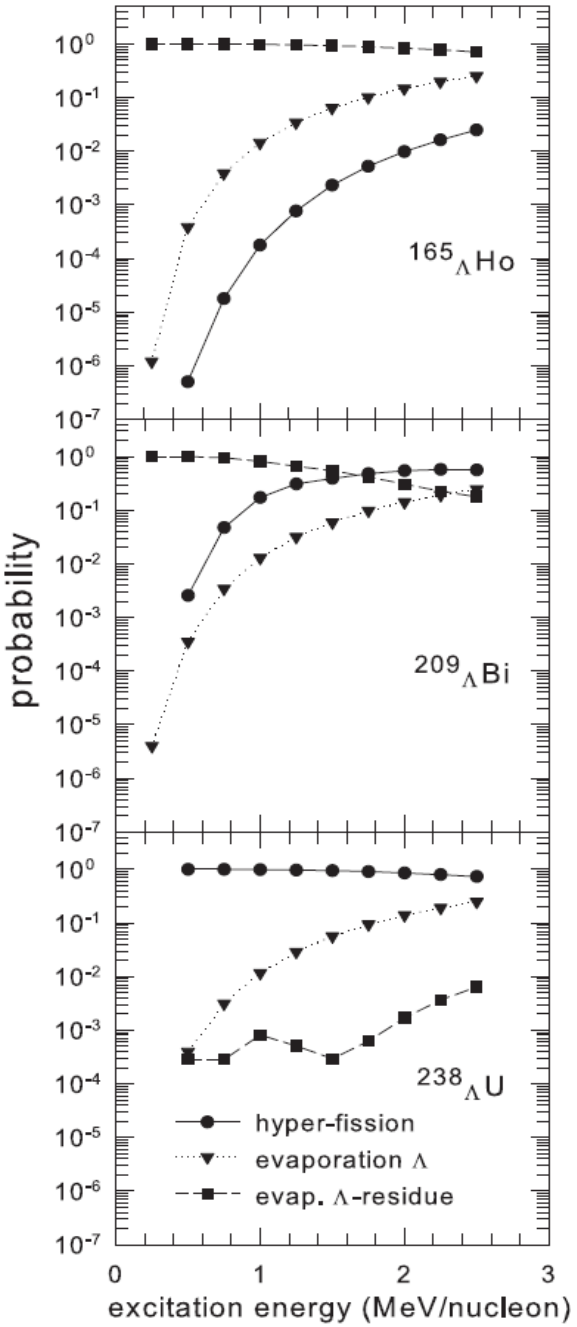

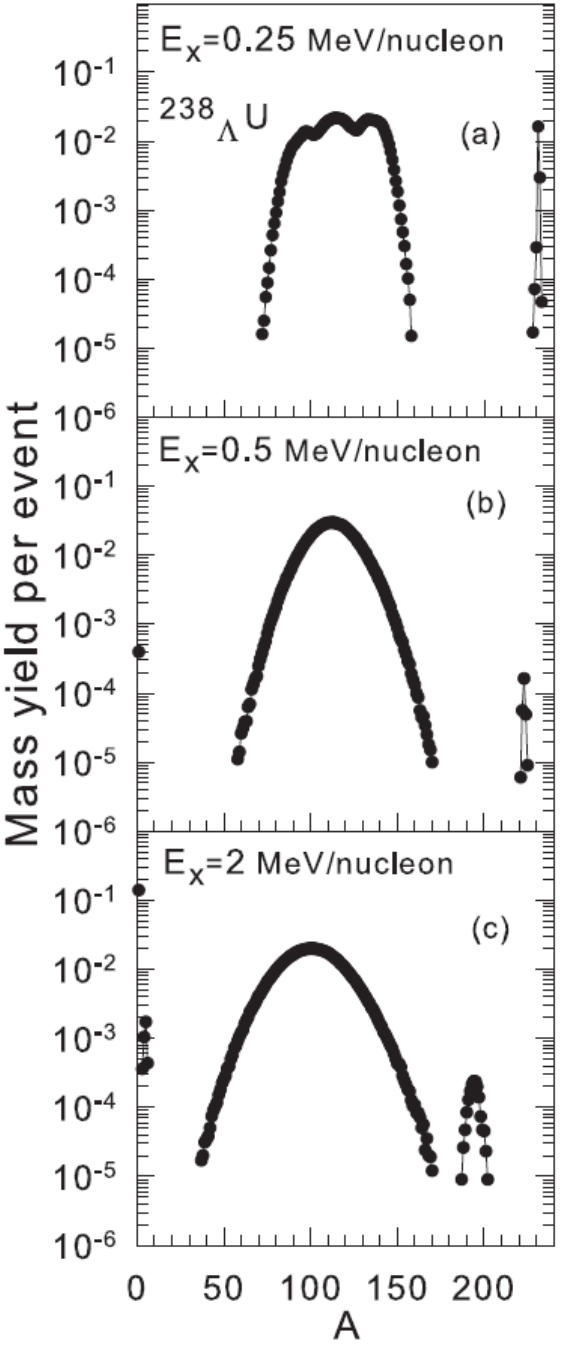

De-excitation of hot light hypernuclear systems

A.Sanchez-Lorente, A.S.Botvina, J.Pochodzalla, Phys. Lett. B697 (2011)222

For light primary fragments (with $A \leq 16$) even a relatively small excitation energy may be comparable with their total binding energy. In this case we assume that the principal mechanism of de-excitation is the explosive decay of the excited nucleus into several smaller clusters (the secondary break-up). To describe this process we use the famous Fermi model [105]. It is analogous to the above-described statistical model, but all final-state fragments are assumed to be in their ground or low excited states. In this case the statistical weight of the channel containing n particles with masses m_i $(i = 1, \ldots, n)$ in volume V_f may be calculated in microcanonical approximation:

$$\Delta\Gamma_f^{\mathrm{mic}} \propto \frac{S}{G}\left(\frac{V_f}{(2\pi\hbar)^3}\right)^{n-1}\left(\frac{\prod_{i=1}^{n} m_i}{m_0}\right)^{3/2}\frac{(2\pi)^{(3/2)(n-1)}}{\Gamma(\frac{3}{2}(n-1))}\left(E_{\mathrm{kin}} - U_f^C\right)^{(3/2)n-5/2}, \qquad (58)$$

where $m_0 = \sum_{i=1}^{n} m_i$ is the mass of the decaying nucleus, $S = \prod_{i=1}^{n}(2s_i + 1)$ is the spin degeneracy factor (s_i is the ith particle spin), $G = \prod_{j=1}^{k} n_j!$ is the particle identity factor (n_j is the number of particles of kind j). E_{kin} is the total kinetic energy of particles at infinity which is related to the prefragment excitation energy E^*_{AZ} as

$$E_{\mathrm{kin}} = E^*_{AZ} + m_0c^2 - \sum_{i=1}^{n} m_ic^2. \qquad (59)$$

U_f^C is the Coulomb interaction energy between cold secondary fragments given by Eq. (49), U_f^C and V_f are attributed now to the secondary break-up configuration.

Generalization of the Fermi-break-up model: new decay channels with hypernuclei were included ; masses and spins of hypernuclei and their excited states were taken from available experimental data and theoretical calculations

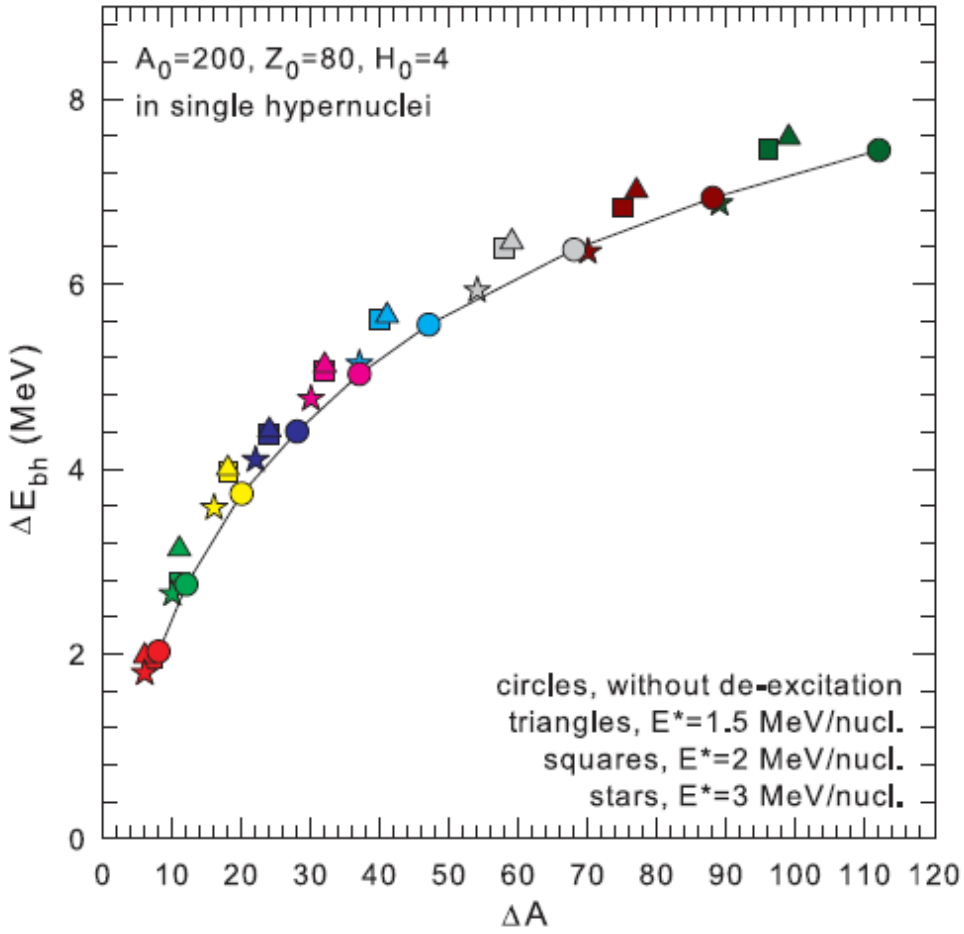

FIG. 4: (Color online) Influence of the secondary de-excitation on the difference of binding energies of hyperons in nuclei $\Delta E_{\rm bh}$ as function of their mass number difference ΔA, by taking single hypernuclei (which are same as in Fig. 2). The calculations of double ratio yields for primary hot nuclei shown for temperature 4 MeV (dashed line, color circle symbols). The triangles, squares, and stars are the calculations with modified double ratios after the secondary de-excitation (via nuclear evaporation) of primary nuclei at excitation energies of 1.5, 2.0, and 3.0 MeV/nucleon, respectively. The same color symbols show the evolution of the results corresponding to the nuclei